Atomic or Molecular Manipulation Involves:

1. Positioning
2. Engaging
3. Displacing
4. Modifying

Manipulation Tools

1. STM
2. AFM
3. Optical
4. Magnetic
5. Mechanical

Scanning Tunneling Microscopy

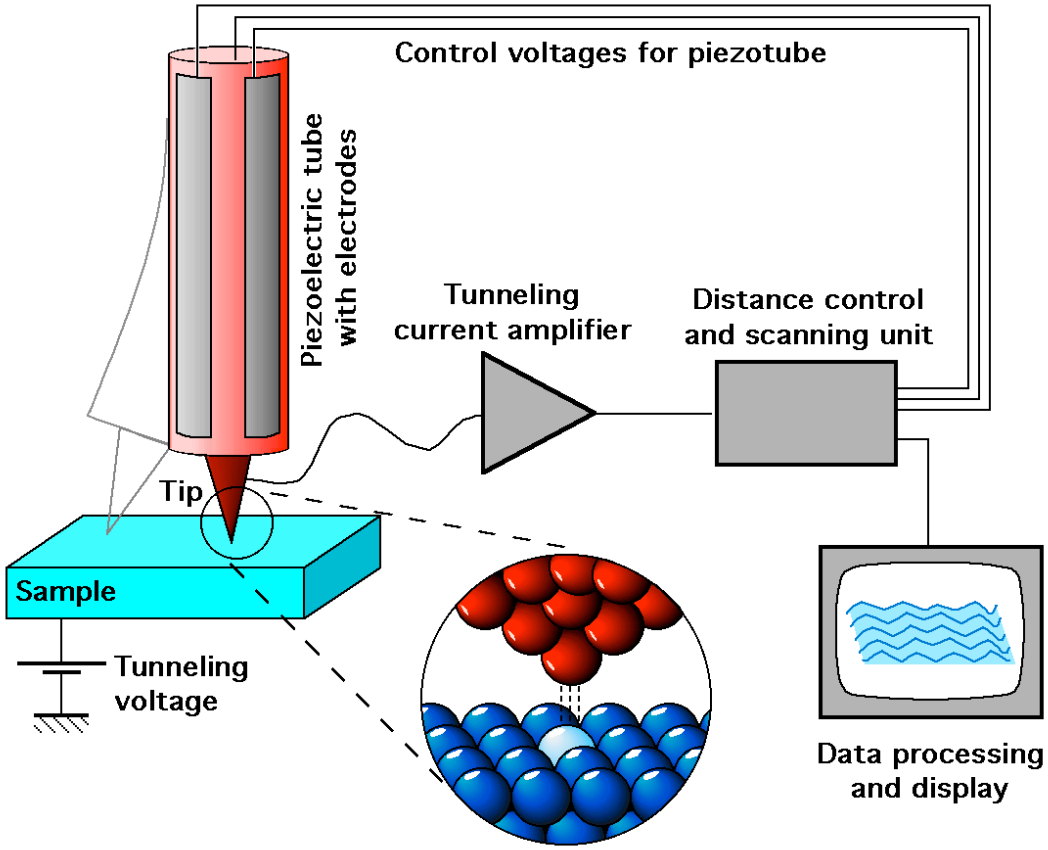

1. G. Binnig, H. Rohrer, C. Gerber, and Weibel, Phys. Rev. Lett. **49**, 57 (1982); and ibid **50**, 120 (1983).
2. J. Chen, *Introduction to Scanning Tunneling Microscopy*, New York, Oxford Univ. Press (1993).

Cu(111) surface at 4K

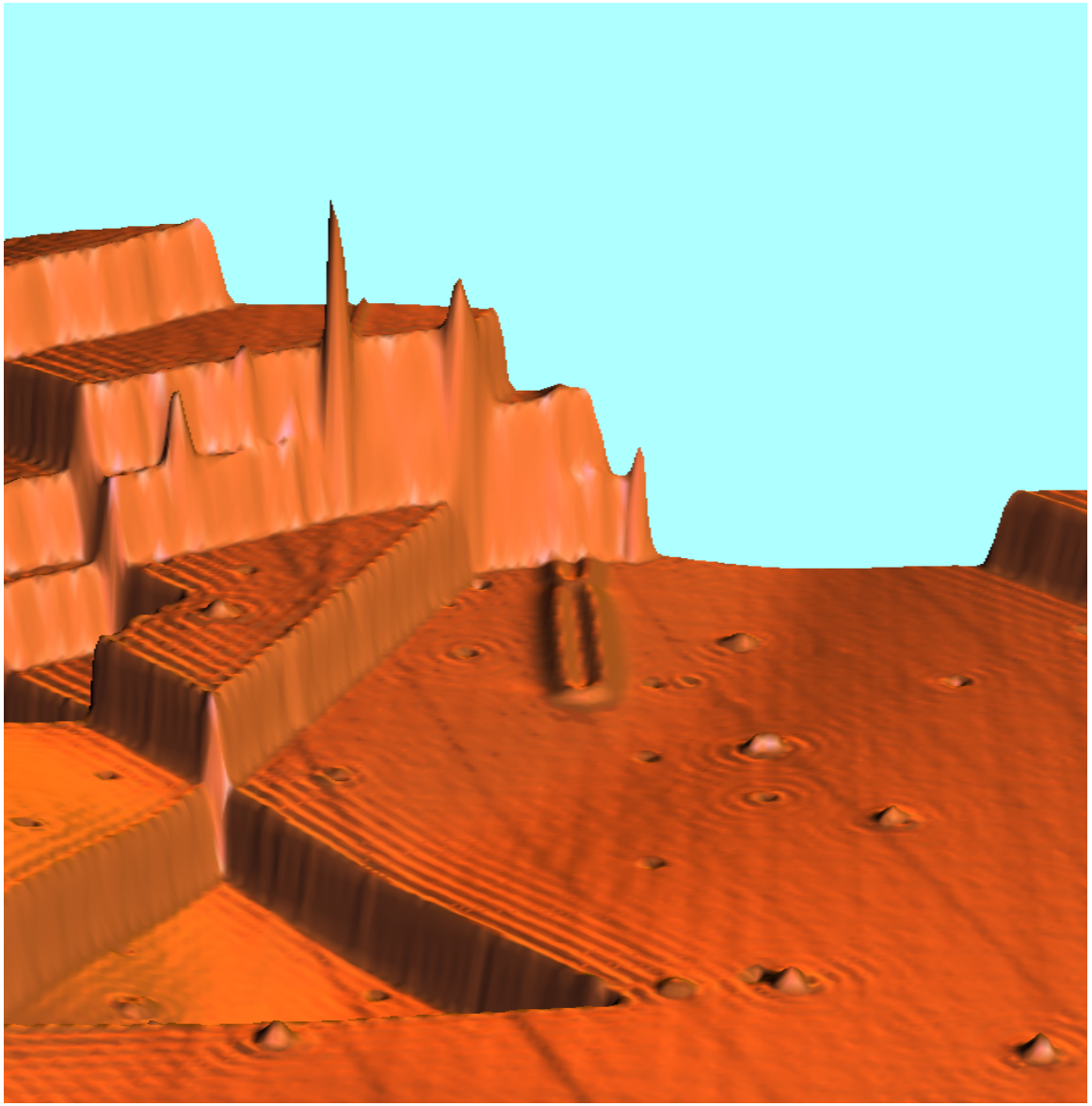

Concept: Eye and Finger

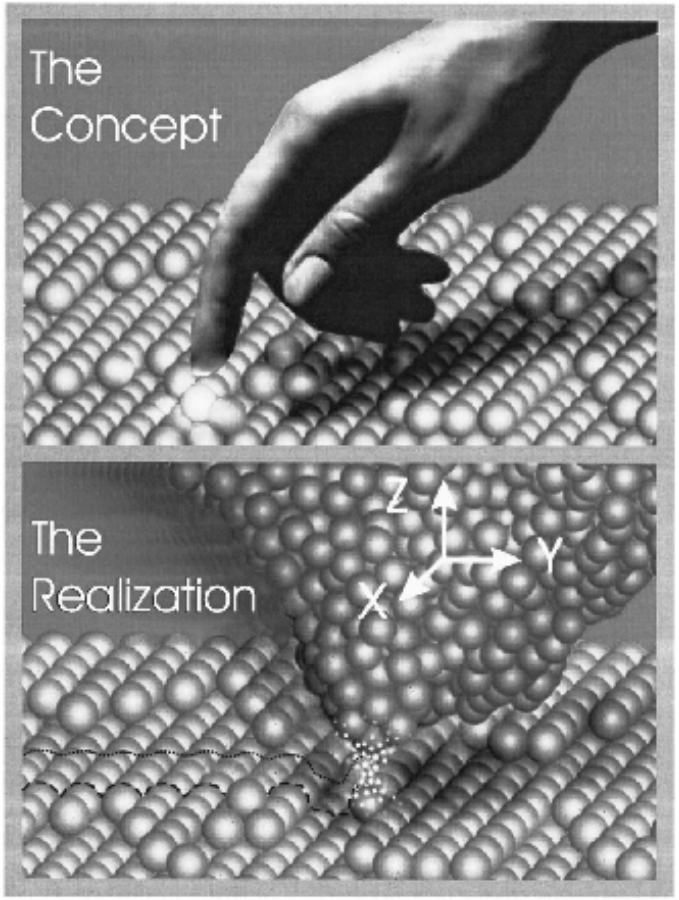

G. Binnig and and H. Rohrer, *Rev. of Mod. Phys.* **71**, S324-S330 (1999).

Atomic Manipulation with STM

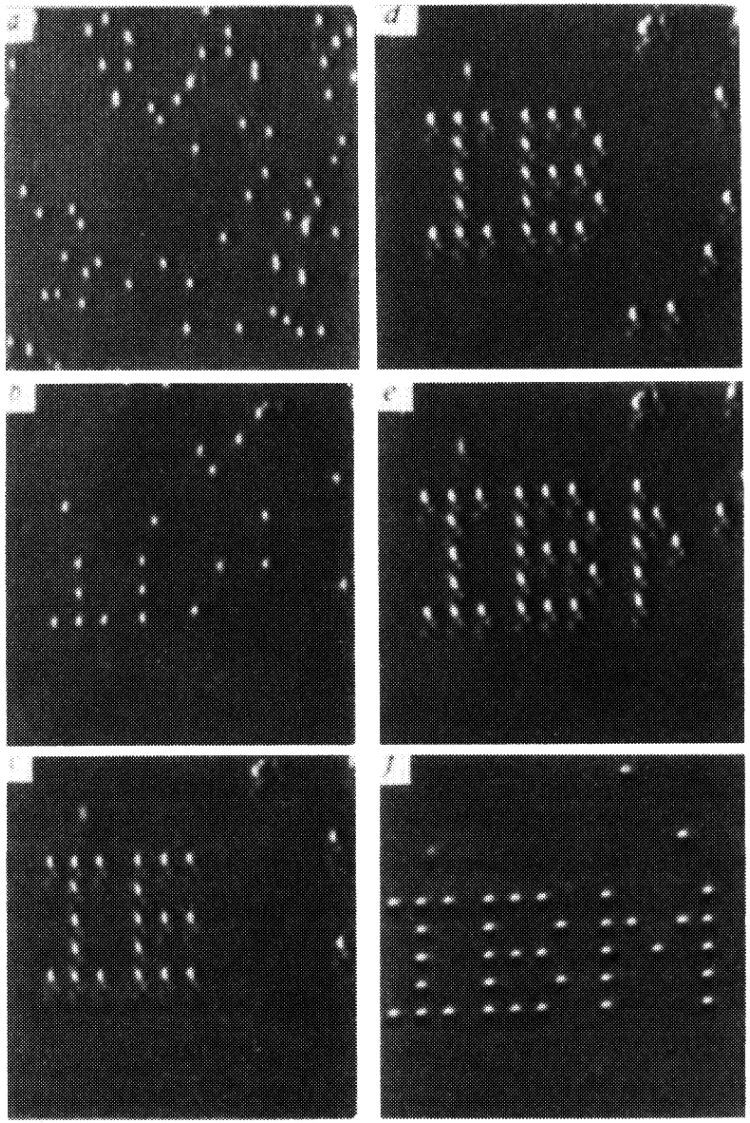

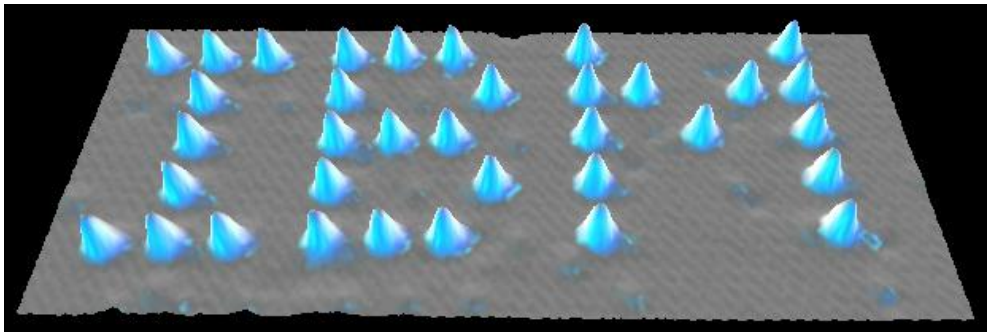

Nature **344**, 524 (1990)

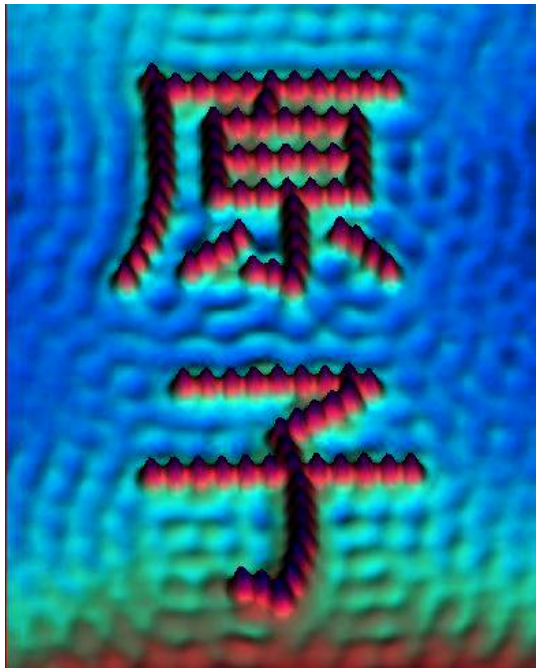

Processes in STM manipulation

A. Lateral movement

1. Sliding
2. Near contact
3. Field induced

B. Vertical movement

1. Transfer
2. Field evaporation
3. Electromigration

J. Stroscio and D. Eigler, Science **254**, 1319 (1991)

Techniques for STM Manipulation

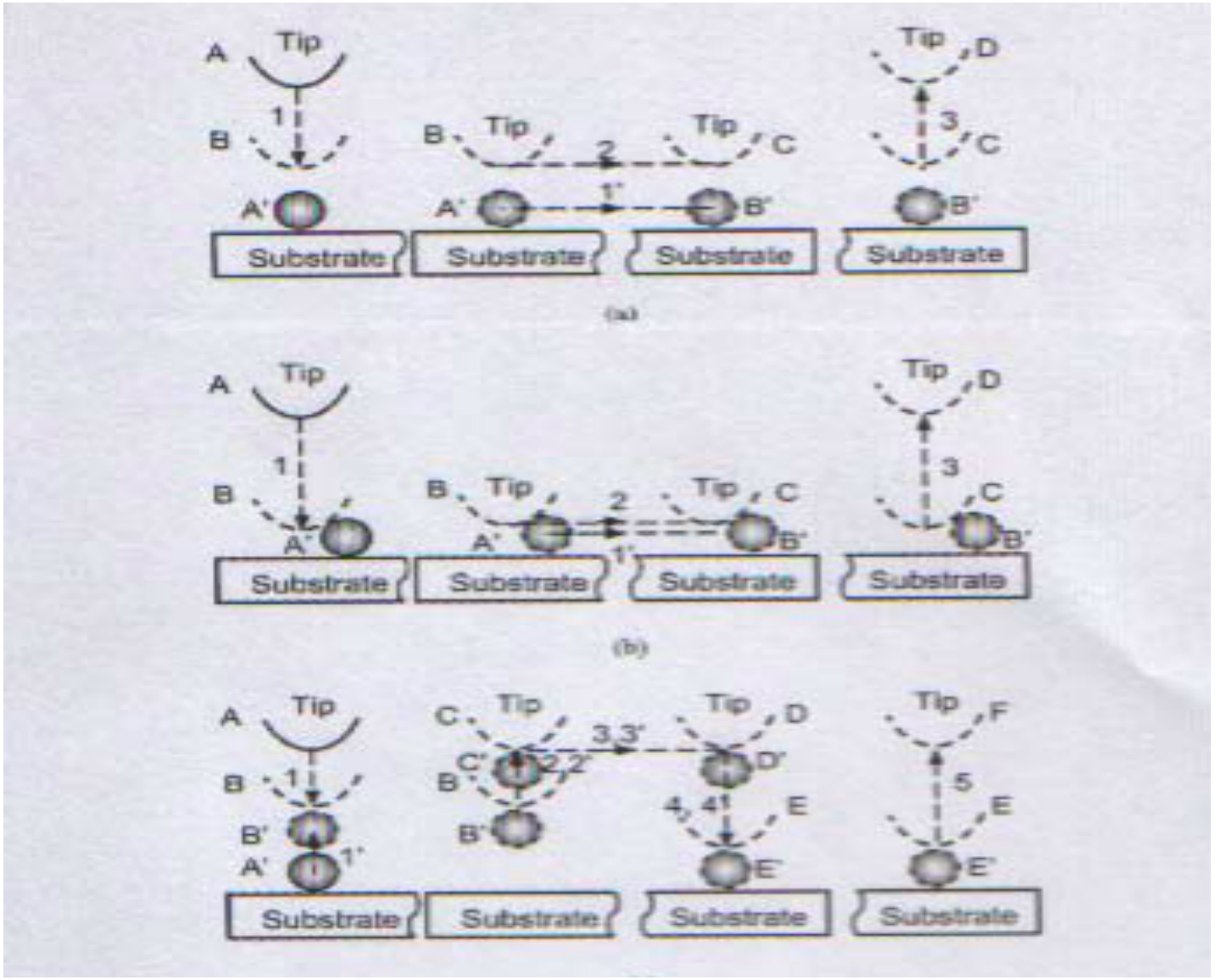

Sliding

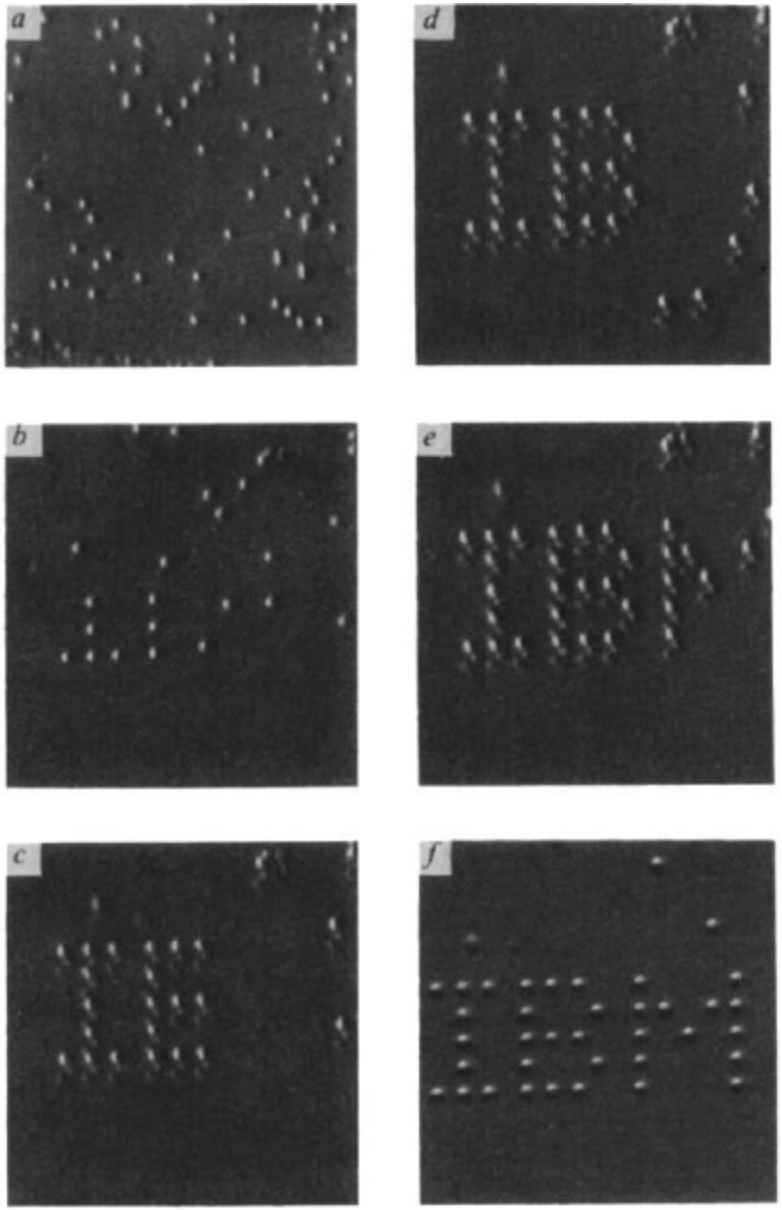

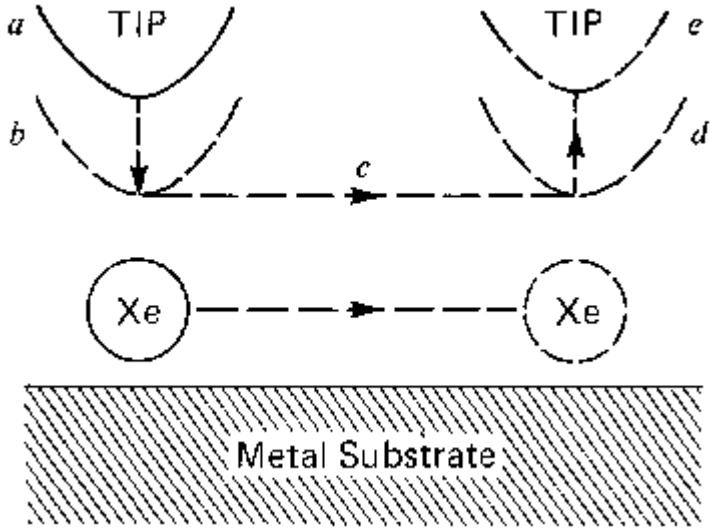

Xe on Ni(110) at 4.5K

D. Eigler et al, *Nature* **344**, 524 (1990)

Quantum Corral

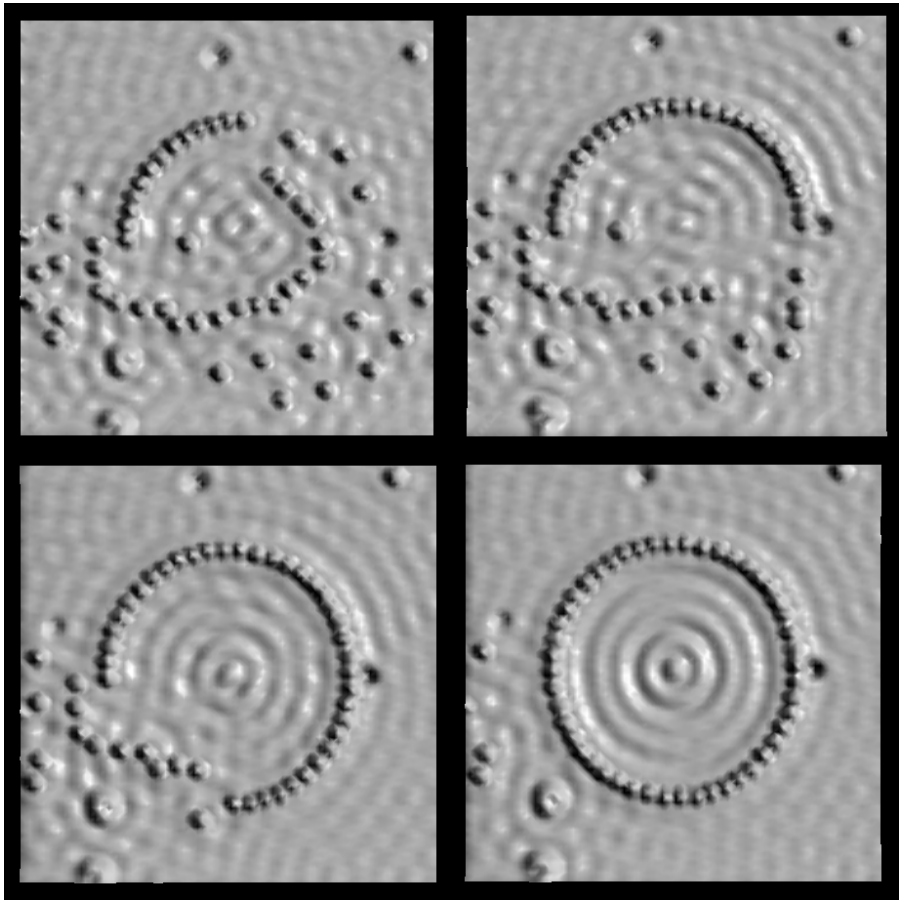

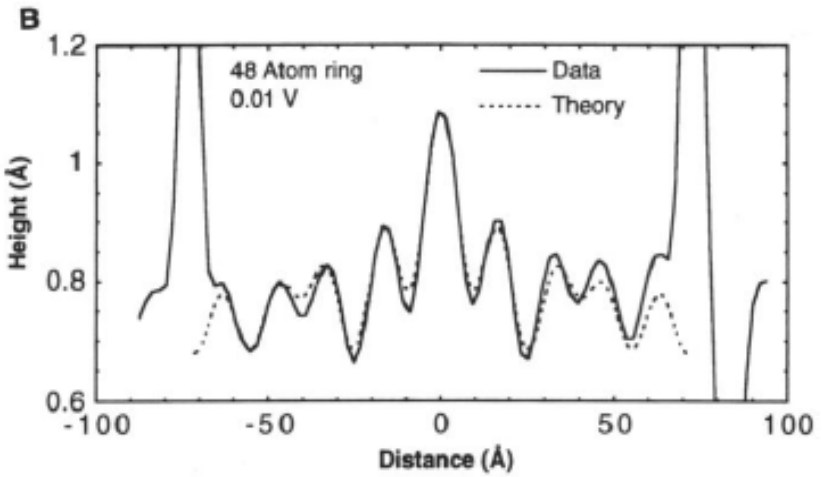

Exp.-theory: **B**) Solid line: cross section of the above data. Dashed line: fit to cross section using a linear combination of |5,0⟩, |4,2⟩, and |2,7⟩ eigenstate densities.

Fe on Cu(111) at 4.5K

M. Crommie et al, *Science* **262**, 218 (1993)

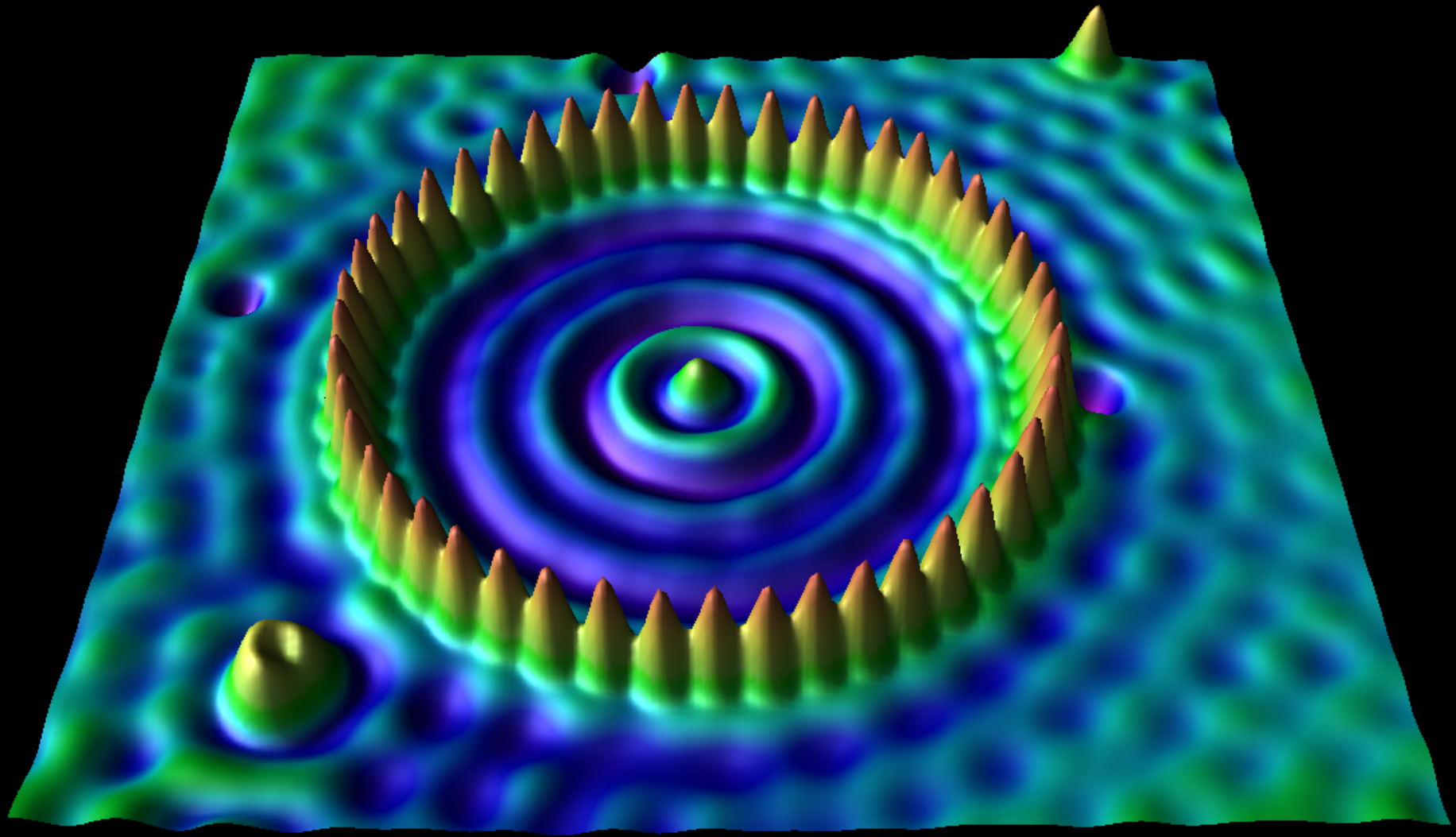

1D Au Atom Chain

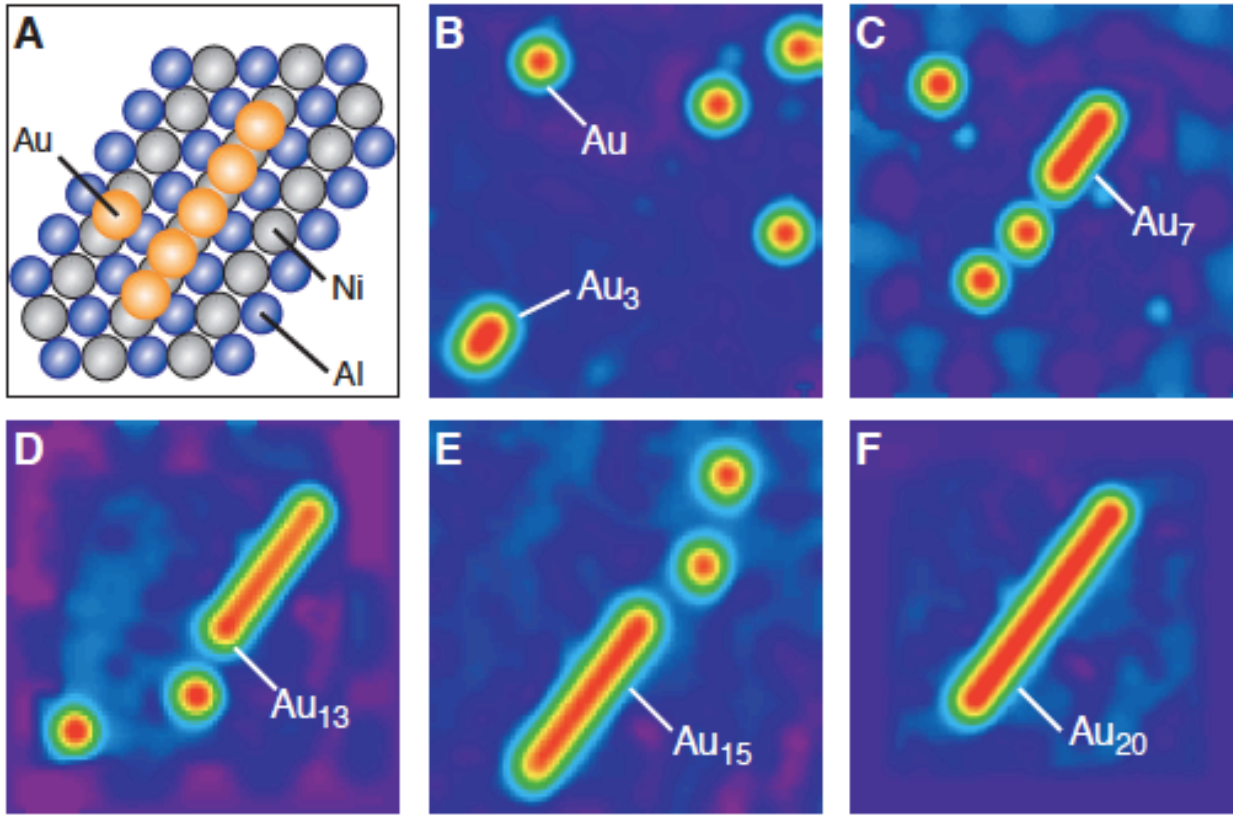

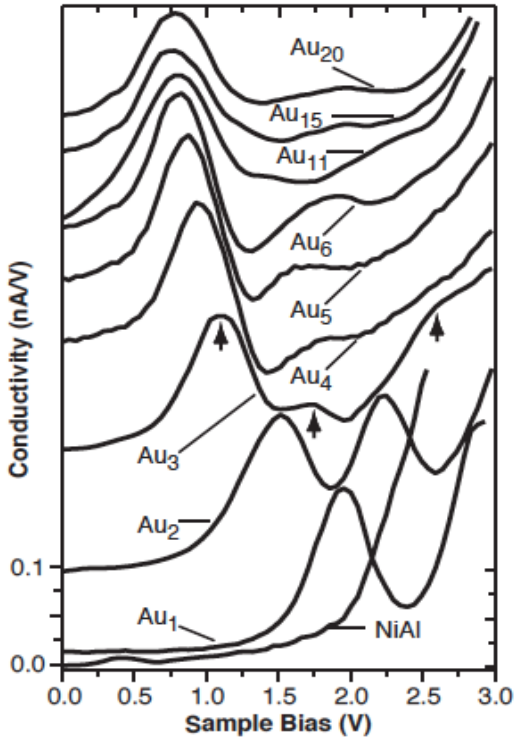

Fig. 2. Conductivity spectra for bare NiAl and for Au chains with different lengths. Spectra were taken in the center of the chains and are offset for clarity. The tunneling gap was set at $V_{sample} = 2.5$ V, $I = 1$ nA. Electronic resonances of Au_3 are marked with arrows.

N. Nilius, T. M. Wallis, W. Ho, *Science* **297**, 1853 (2002)

Detecting Kondo Resonance

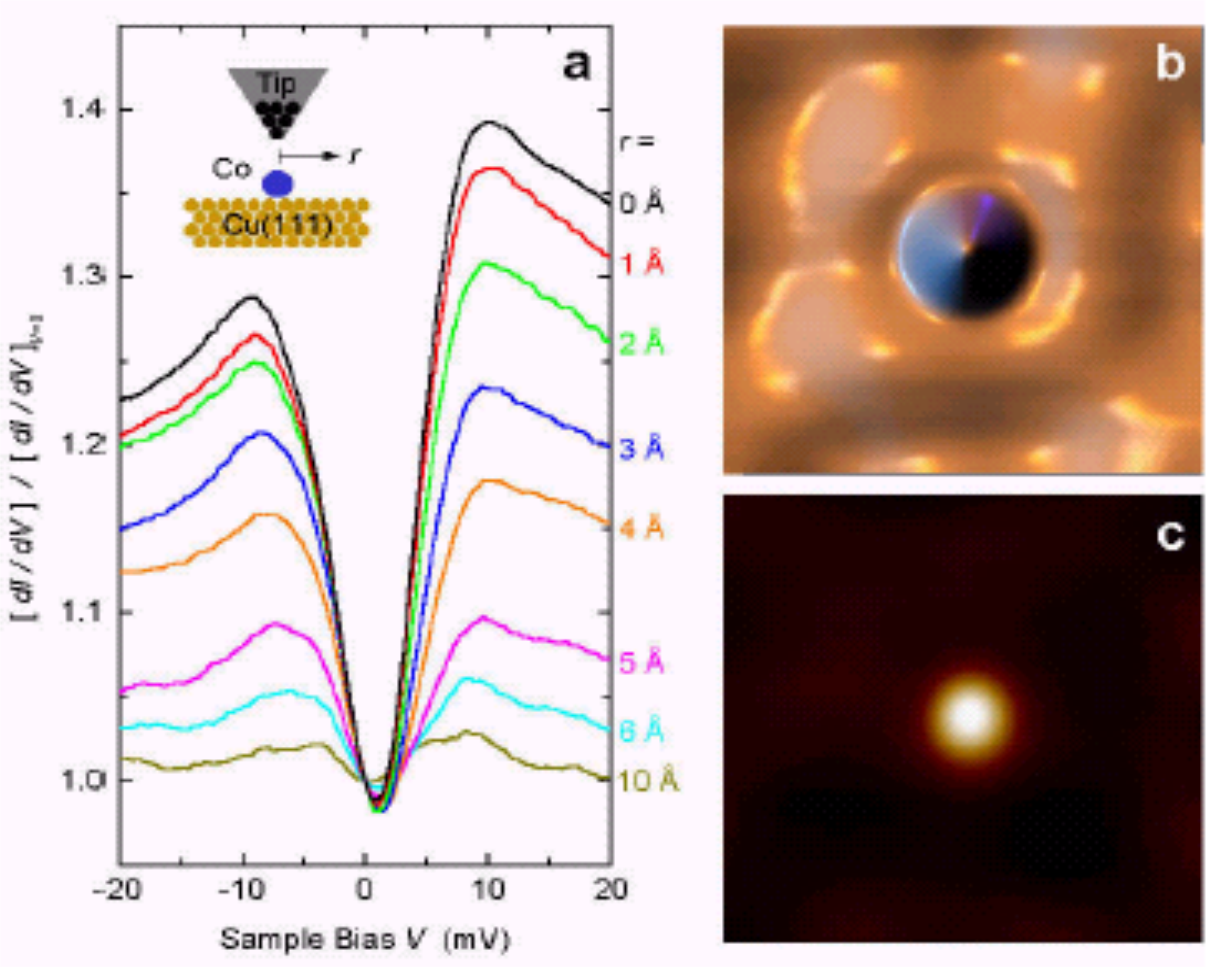

Manoharan, Lutz, and Eigler, *Nature* **403**, 512.515 (2000)

Assembly of elliptical resonators

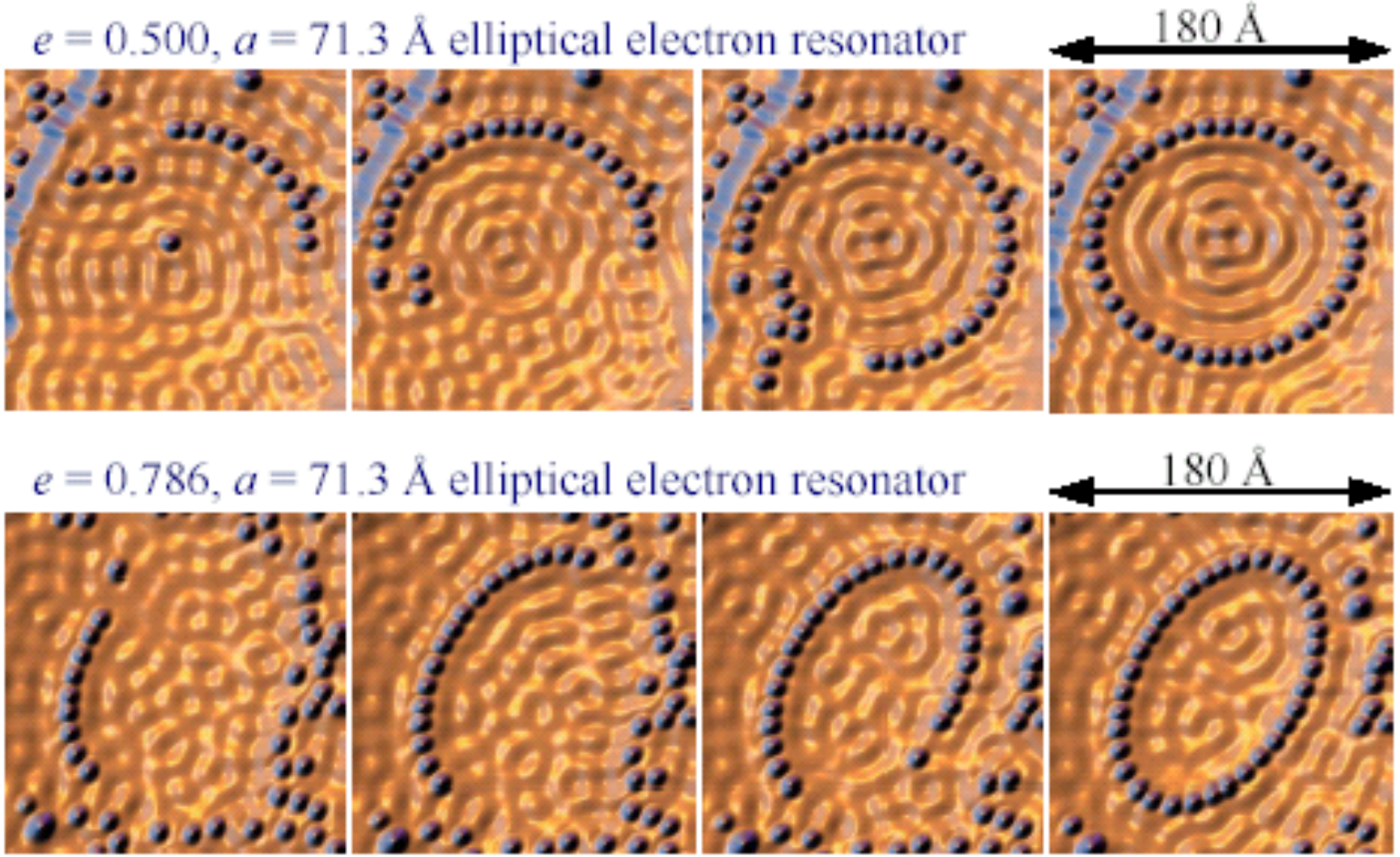

Manoharan, Lutz, and Eigler, *Nature* **403**, 512.515 (2000)

Eigenmodes of elliptical resonator

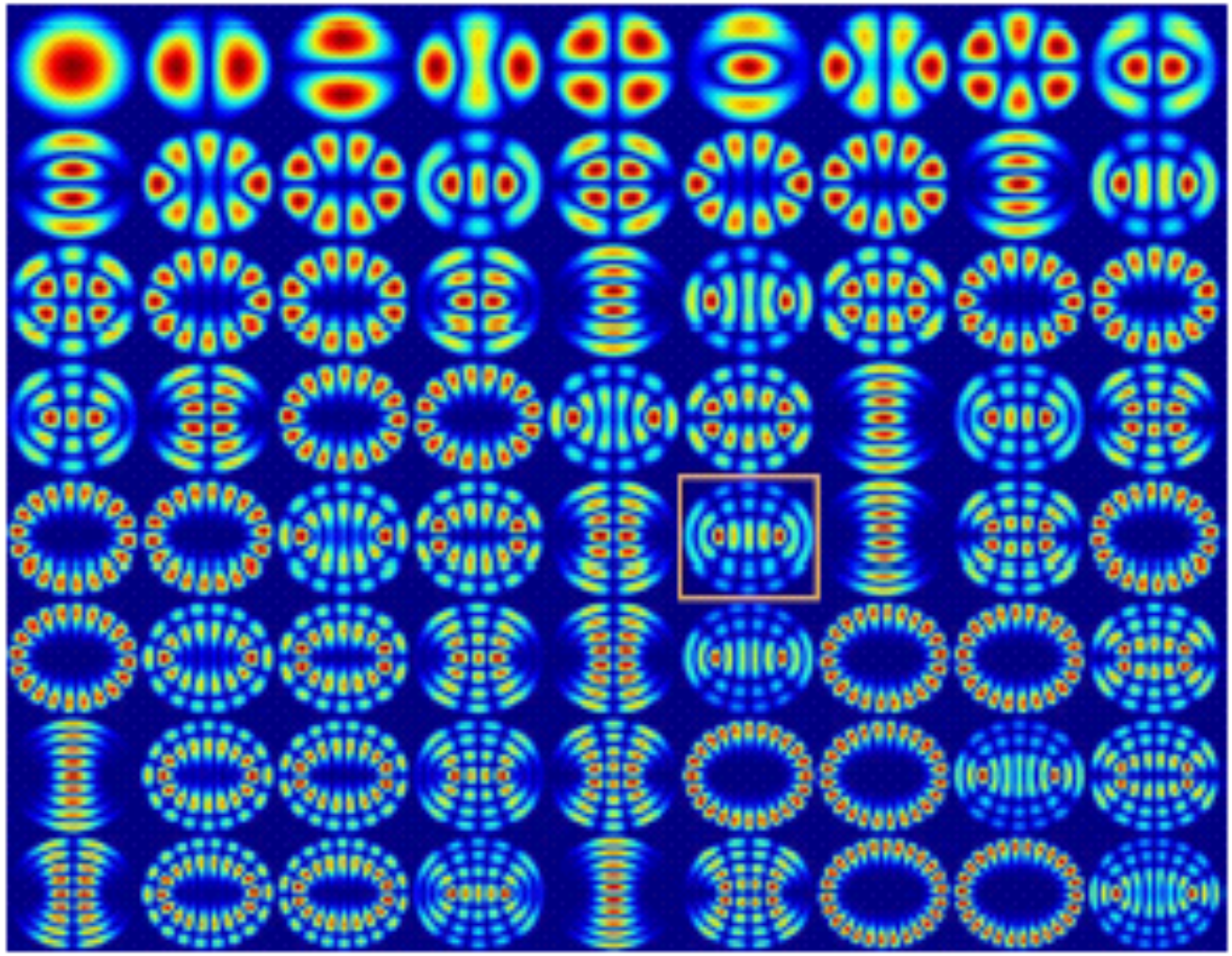

Manoharan, Lutz, and Eigler, *Nature* **403**, 512.515 (2000)

Moving an atom in an elliptical resonator

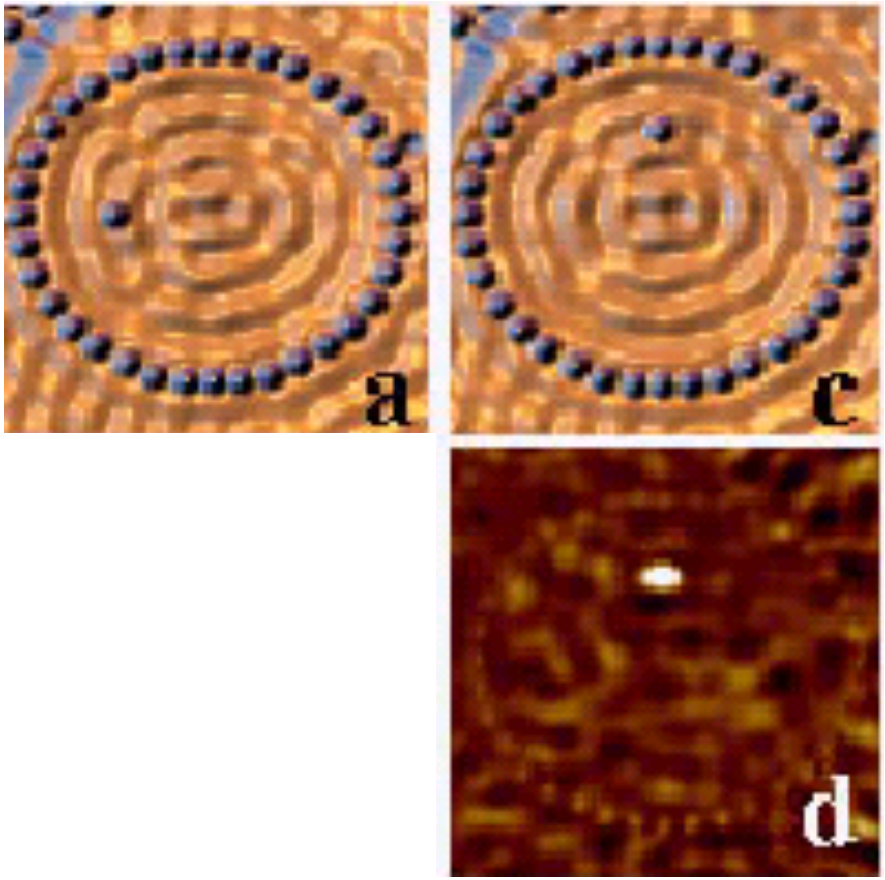

Manoharan, Lutz, and Eigler, *Nature* **403**, 512.515 (2000)

Detection of Quantum Mirage

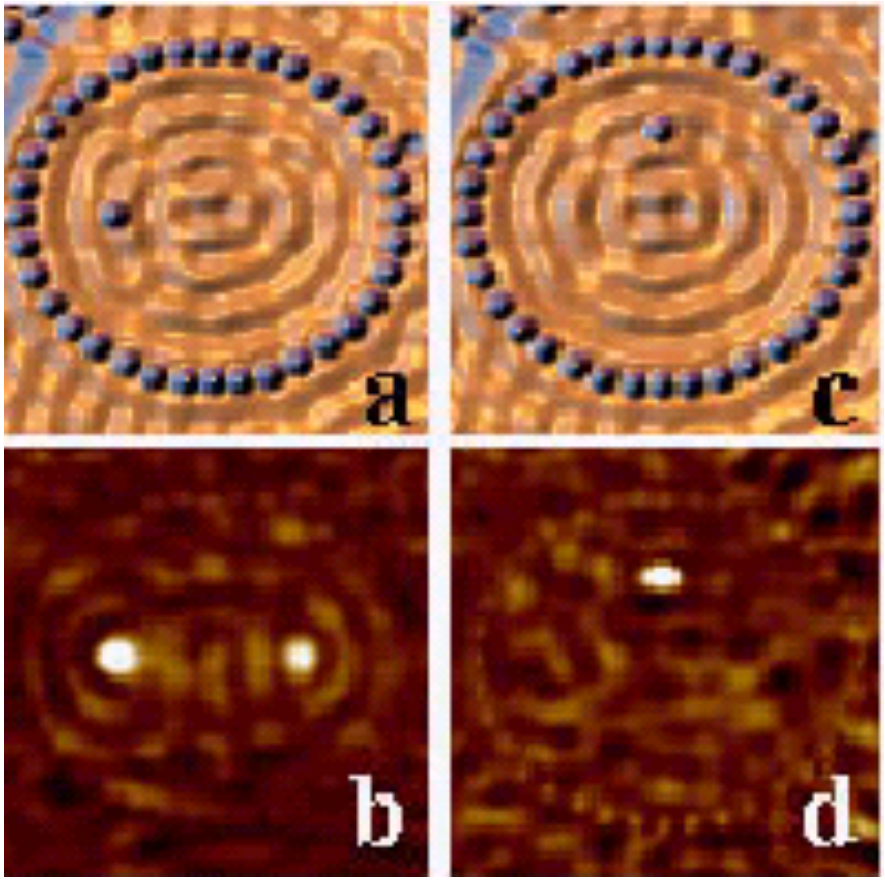

Manoharan, Lutz, and Eigler, *Nature* **403**, 512.515 (2000)

Quantum Mirage

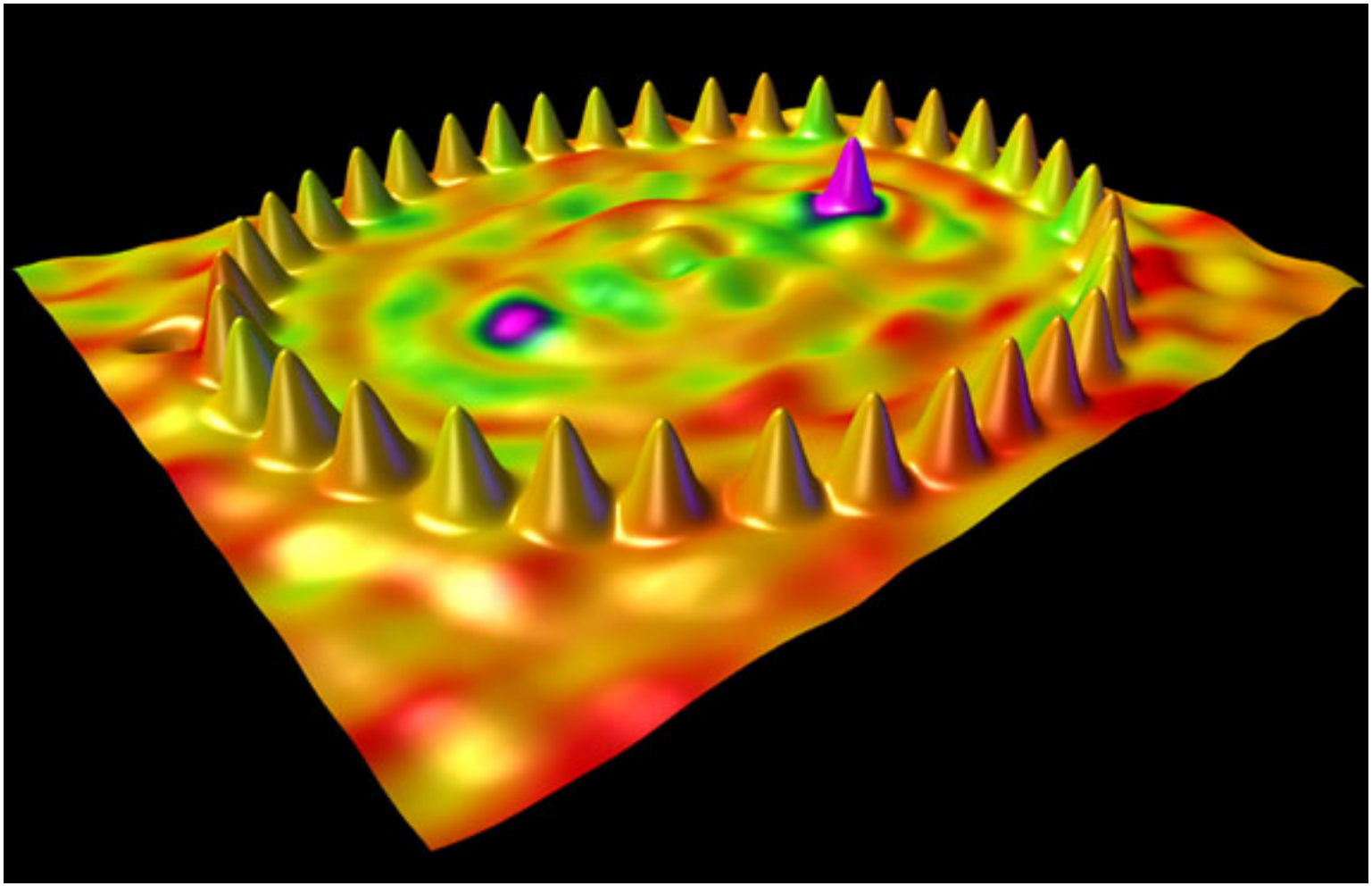

H. C. Manoharan *et al., Nature* 403, 512 (2000).

A molecular cascade device

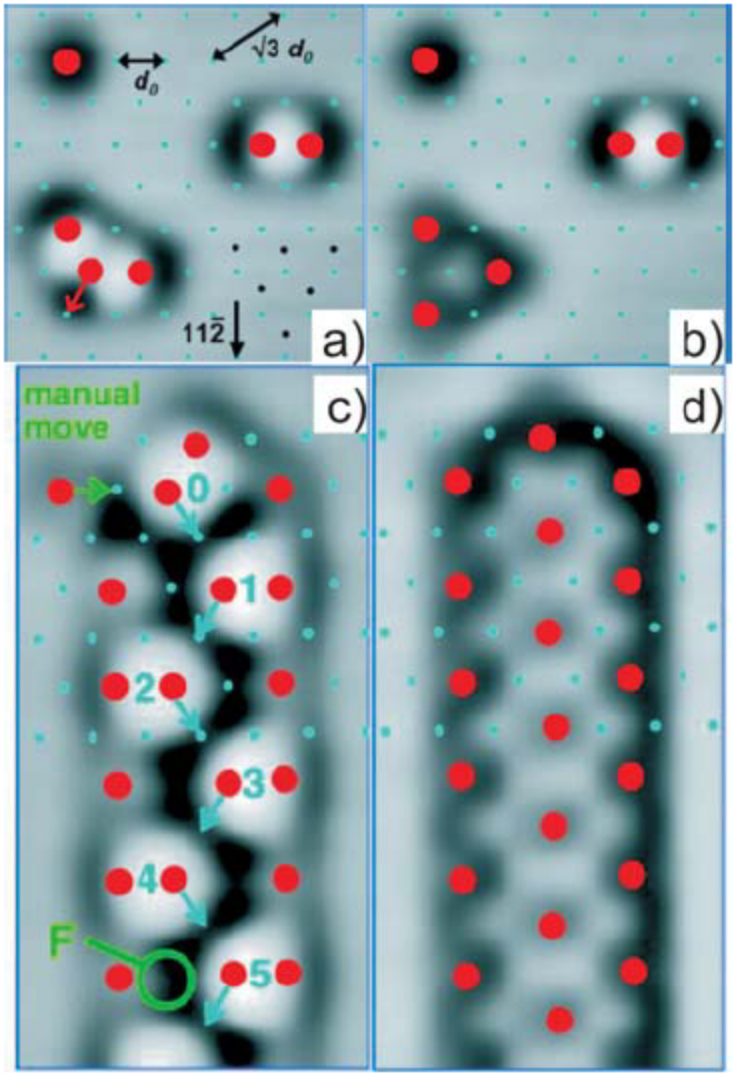

A prototype for a molecular cascade device. CO molecules are deposited on a Cu(111) surface at 4 K. Individual molecules are imaged as depressions (a). The red dots mark adsorption sites for CO molecules, whereas the blue dots represent the lattice positions of Cu atoms.

There are two possible geometries for CO trimers: the chevron configuration (lower left corner of part a) and the threefold symmetric (lower left corner of part b). The chevron trimer is only metastable and decays into the threefold symmetric by displacing the central CO molecule to a nearest-neighbor site (from a to b). By suitably arranging the CO molecules, the decay of one of the trimers into the other one can produce a cascade of events that communicates a bit of information (presence/ absence of a CO molecule at a given site) from one end of the chain to the other (c and d).

A.J.Heinrich et al, *Science* **298**, 1381 (2002)

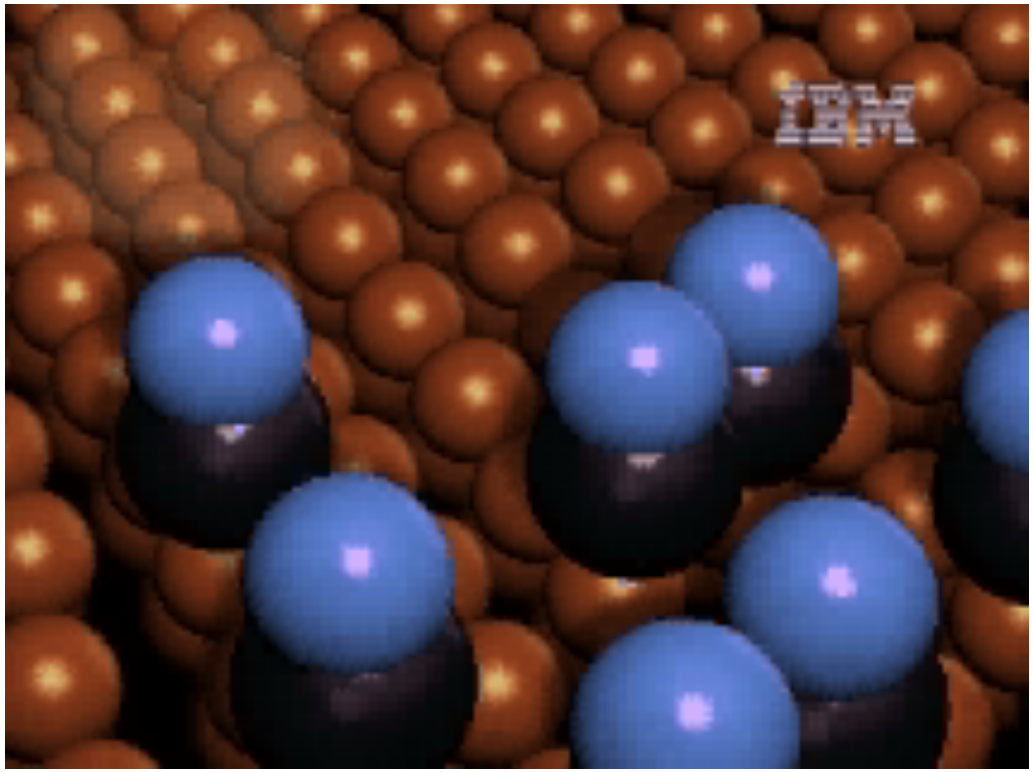
IBM

Sliding molecules at RT

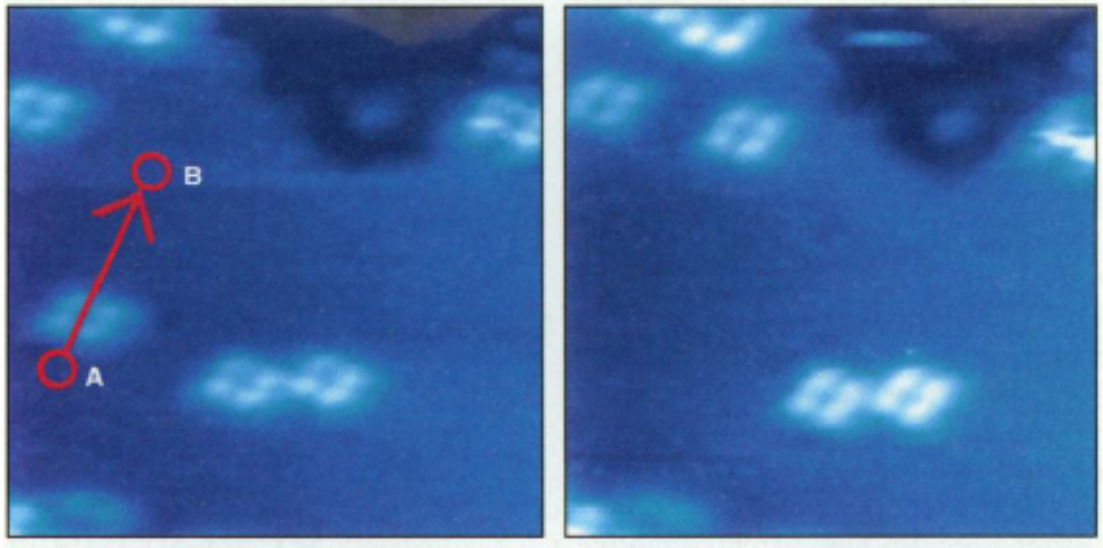

Cu-TP porphyrinon Cu(100)
RT UHV STM

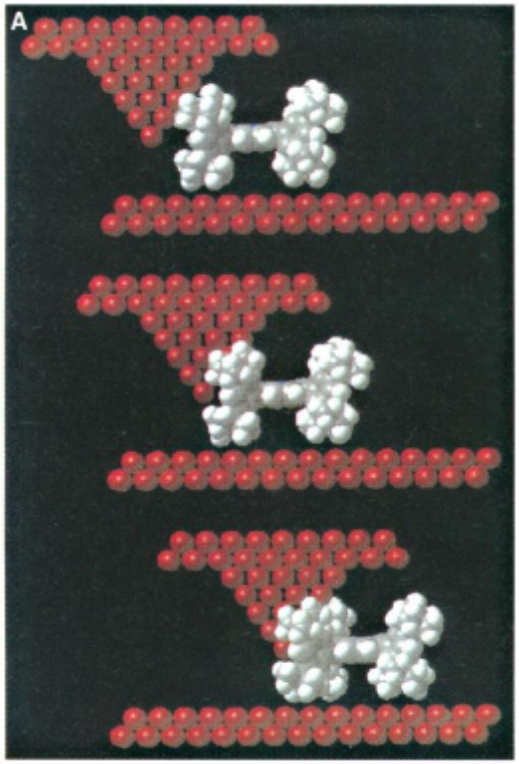

Cu-TBP porphyrin

T.A. Jung et al, *Science* **271**, 181 (1996)

Influence of Molecules on Metals

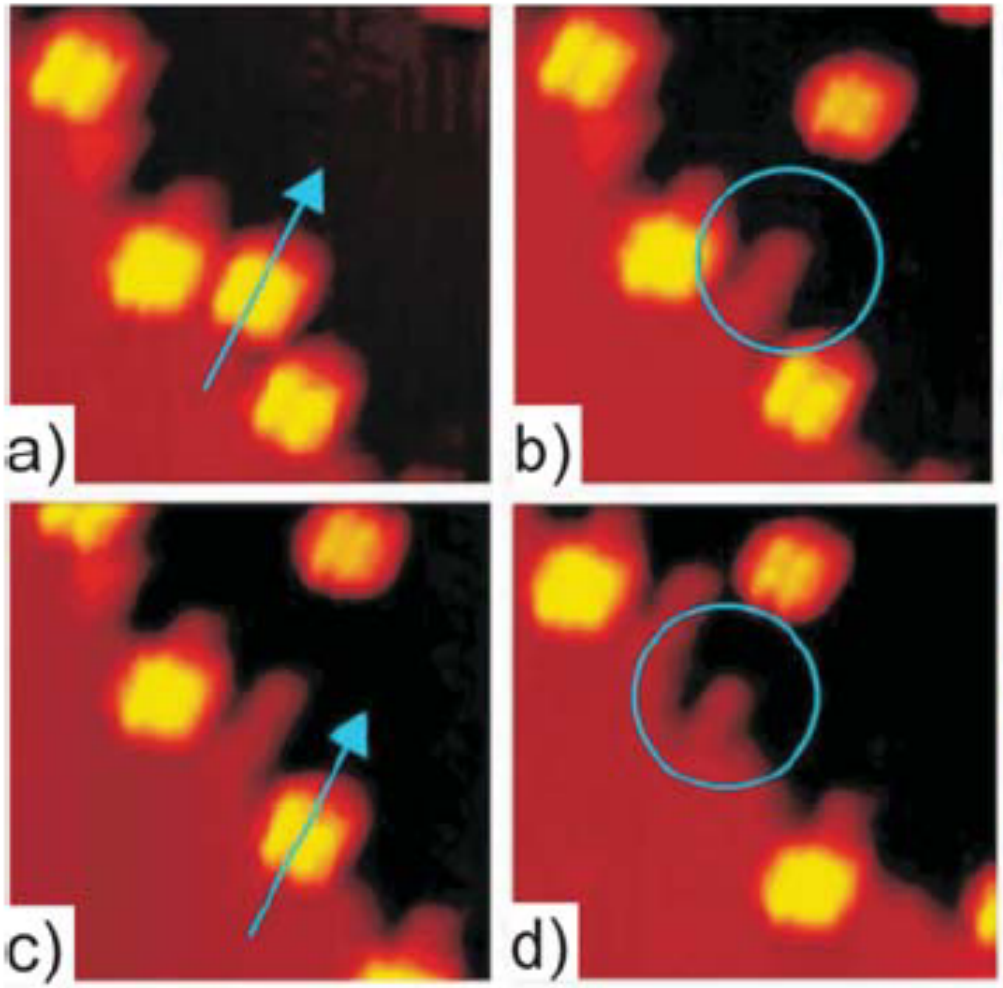

Lander molecule, deposited at RT on Cu(110), imaged at 150K, UHV STM

F. Rosei et al, *Science* **296**, 328 (2002)

Controlling Chemical Reactions

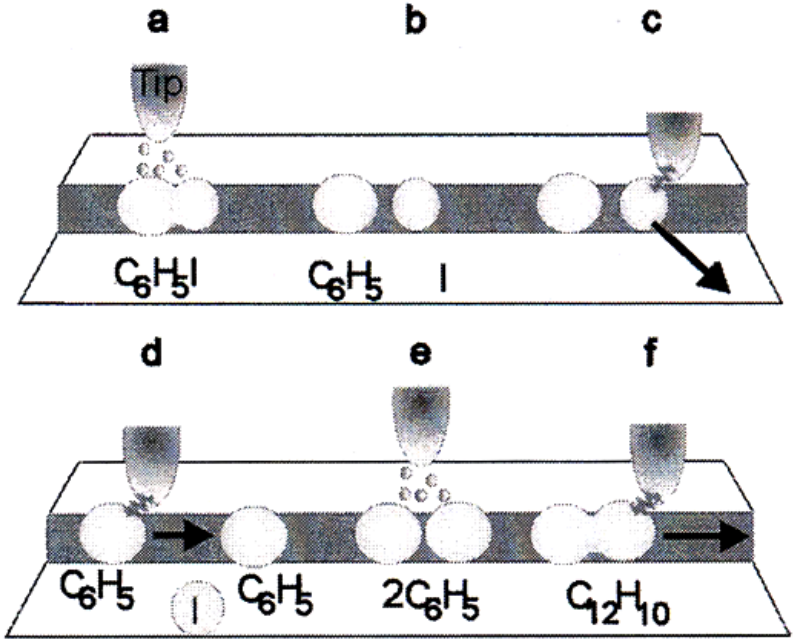

FIG. 1. Schematic illustration of the STM tip-induced synthesis steps of a biphenyl molecule. (a),(b) Electron-induced selective abstraction of iodine from iodobenzene. (c) Removal of the iodine atom to a terrace site by lateral manipulation. (d) Bringing together two phenyls by lateral manipulation. (e) Electron-induced chemical association of the phenyl couple to biphenyl. (f) Pulling the synthesized molecule by its front end with the STM tip to confirm the association.

Rieder Group, *Phys. Rev. Lett.* **85**, 2777 (2000)

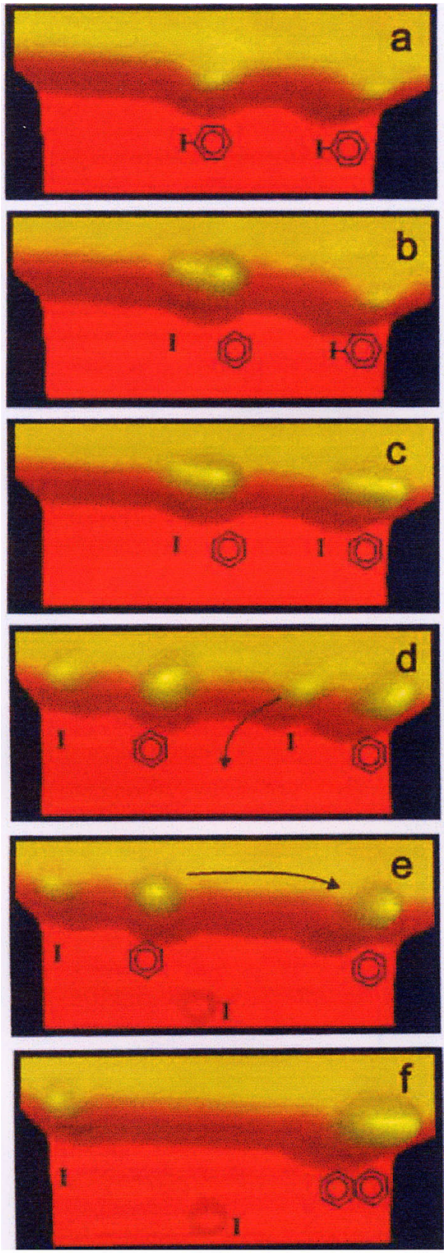

Field-Assisted Diffusion

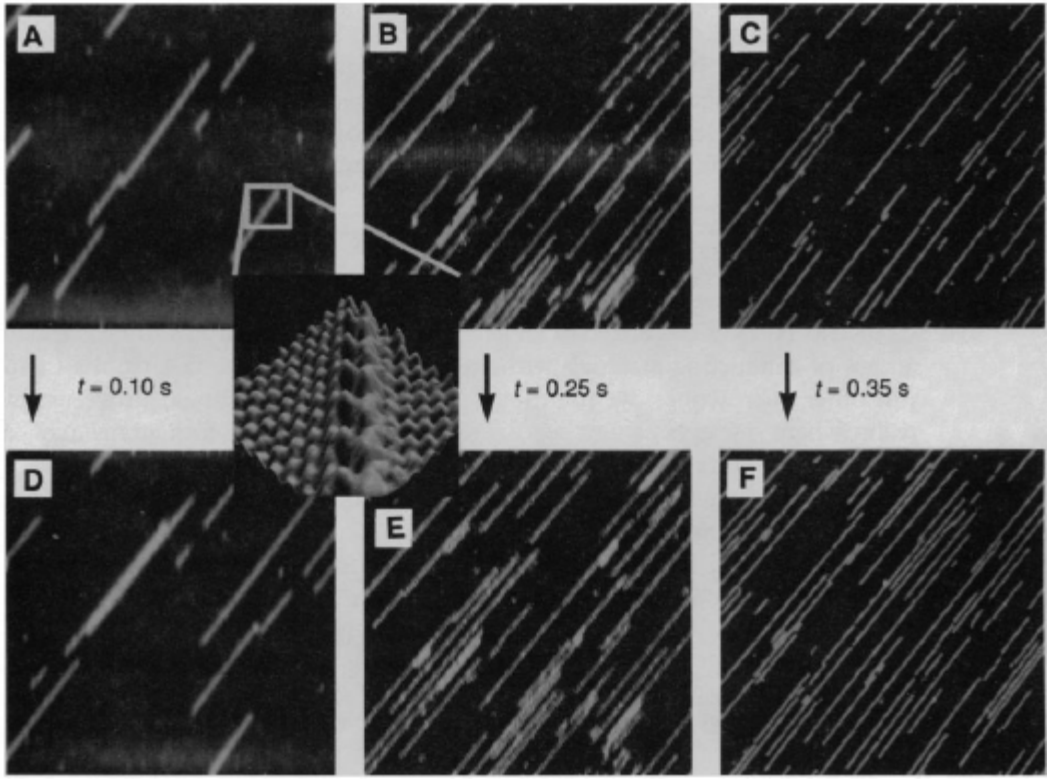

Fig. 2. STM images of Cs on *p*-type GaAs(110) surfaces. (**A** through **C**) Images recorded at −2-V sample bias showing the initial state before pulsing the voltage. The inset in (A) shows an atomic resolution 70 Å by 70 Å image of the Cs zigzag structure on GaAs(110). (**D** through **F**) Images recorded at −2.5 V after pulsing the sample voltage to +1 V, with the tip positioned in the center of the image for 0.15, 0.25, and 0.35 s, respectively. All of the images are 1400 Å by 1400 Å, except (A) and (D), which are 1000 Å by 1000 Å.

L.J. Whitman et al, *Science* **251**, 1206 (1991)

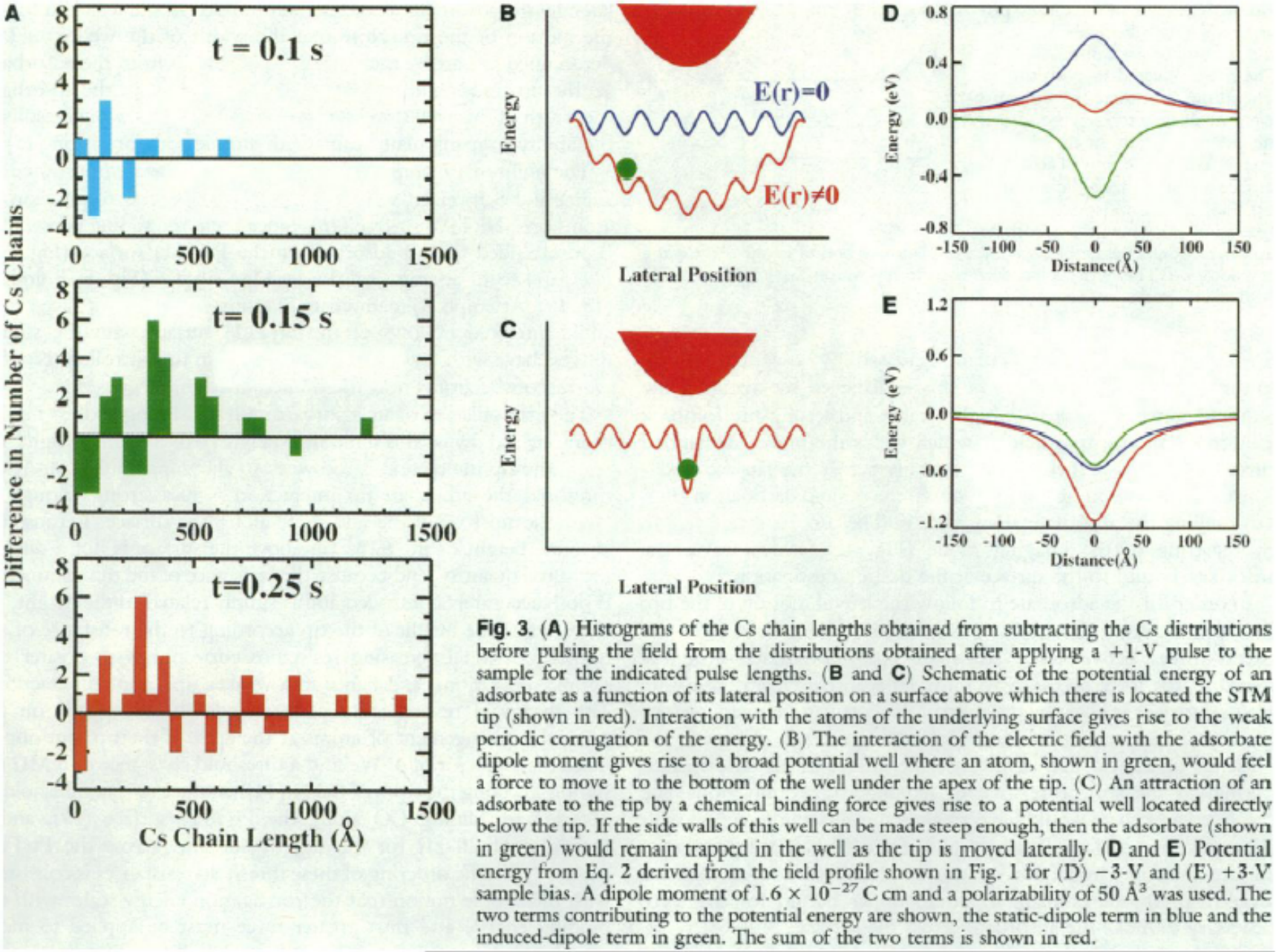

Fig. 3. (**A**) Histograms of the Cs chain lengths obtained from subtracting the Cs distributions before pulsing the field from the distributions obtained after applying a +1-V pulse to the sample for the indicated pulse lengths. (**B** and **C**) Schematic of the potential energy of an adsorbate as a function of its lateral position on a surface above which there is located the STM tip (shown in red). Interaction with the atoms of the underlying surface gives rise to the weak periodic corrugation of the energy. (B) The interaction of the electric field with the adsorbate dipole moment gives rise to a broad potential well where an atom, shown in green, would feel a force to move it to the bottom of the well under the apex of the tip. (C) An attraction of an adsorbate to the tip by a chemical binding force gives rise to a potential well located directly below the tip. If the side walls of this well can be made steep enough, then the adsorbate (shown in green) would remain trapped in the well as the tip is moved laterally. (**D** and **E**) Potential energy from Eq. 2 derived from the field profile shown in Fig. 1 for (D) −3-V and (E) +3-V sample bias. A dipole moment of 1.6×10^{-27} C cm and a polarizability of 50 $Å^3$ was used. The two terms contributing to the potential energy are shown, the static-dipole term in blue and the induced-dipole term in green. The sum of the two terms is shown in red.

Transfer of a molecule

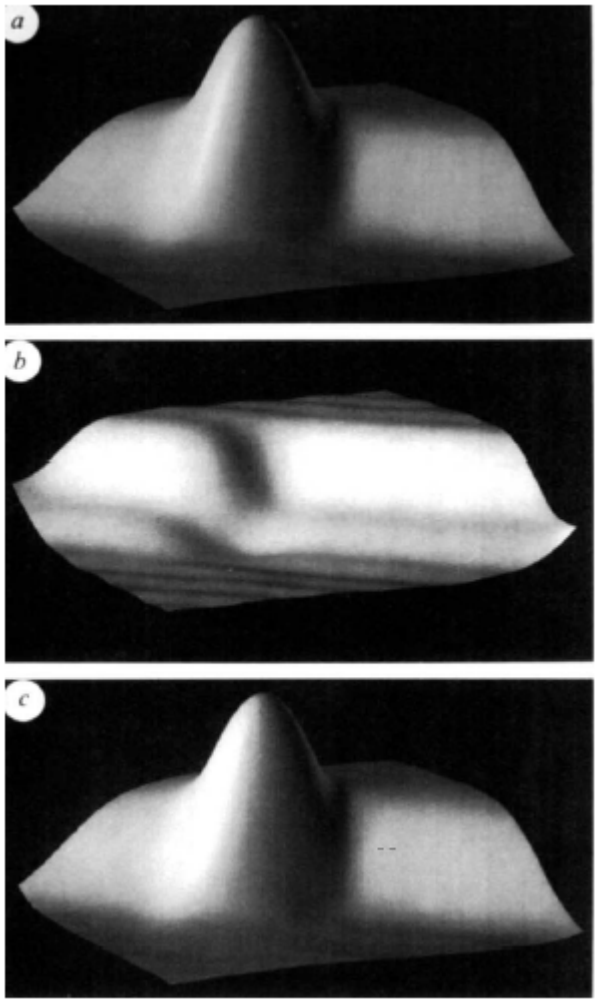

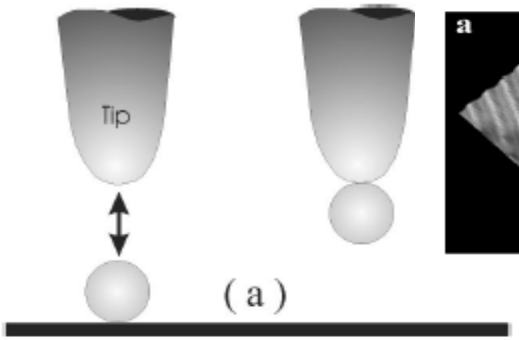

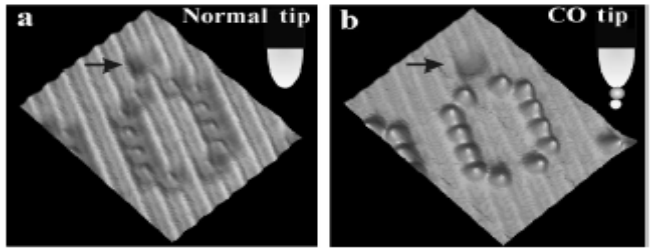

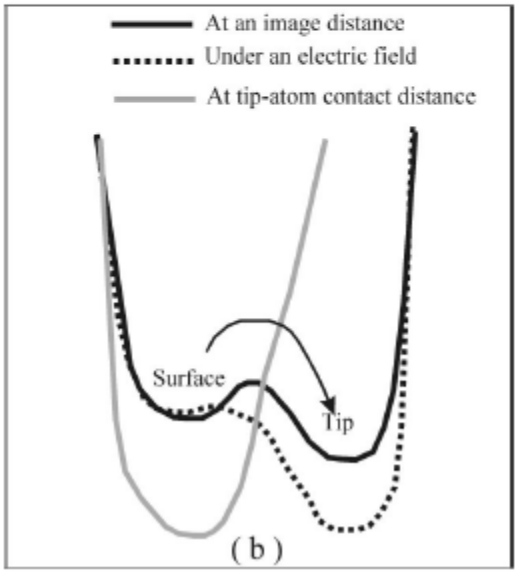

J. Repp,

Rieder Group, Berlin

G. Meyer et al.,
Single Mol. **1,** 79 (2000)

D. Eigler et al, *Nature* **352**, 600 (1991)

Field Evaporation

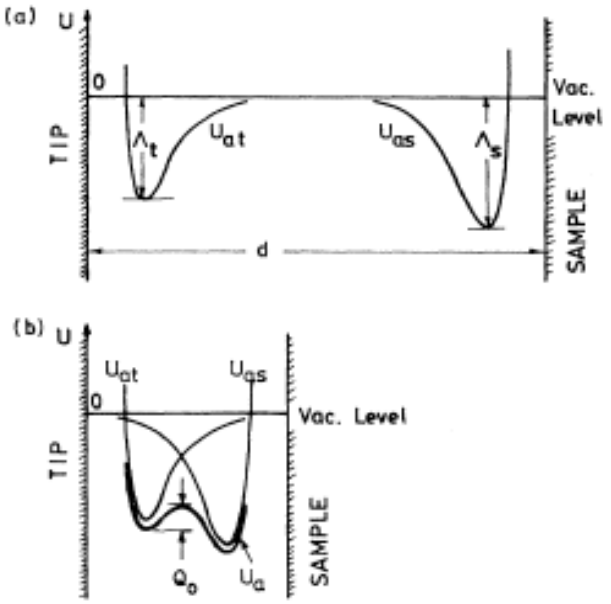

FIG. 1. When the tip to sample distance d is large, the atom-tip and atom-sample interactions U_{at} and U_{as} do not overlap significantly as shown in (a). When d is small, the two start to overlap and U_a, which is the sum of U_{at} and U_{as}, exhibits a double-well structure having a small activation barrier. The atom can either be transferred from the tip to the sample or from the sample to the tip, as shown in (b).

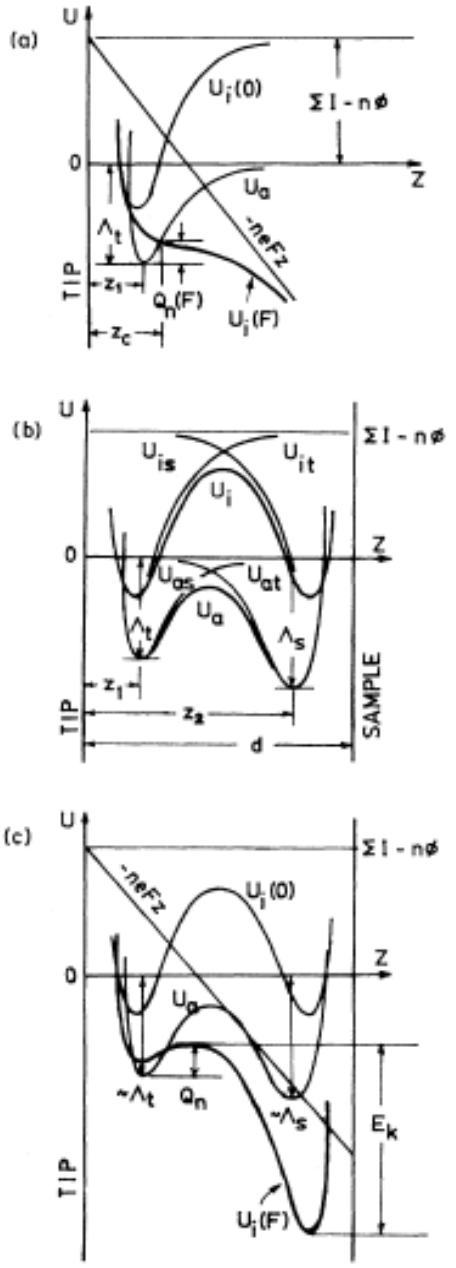

Golden Taiwan

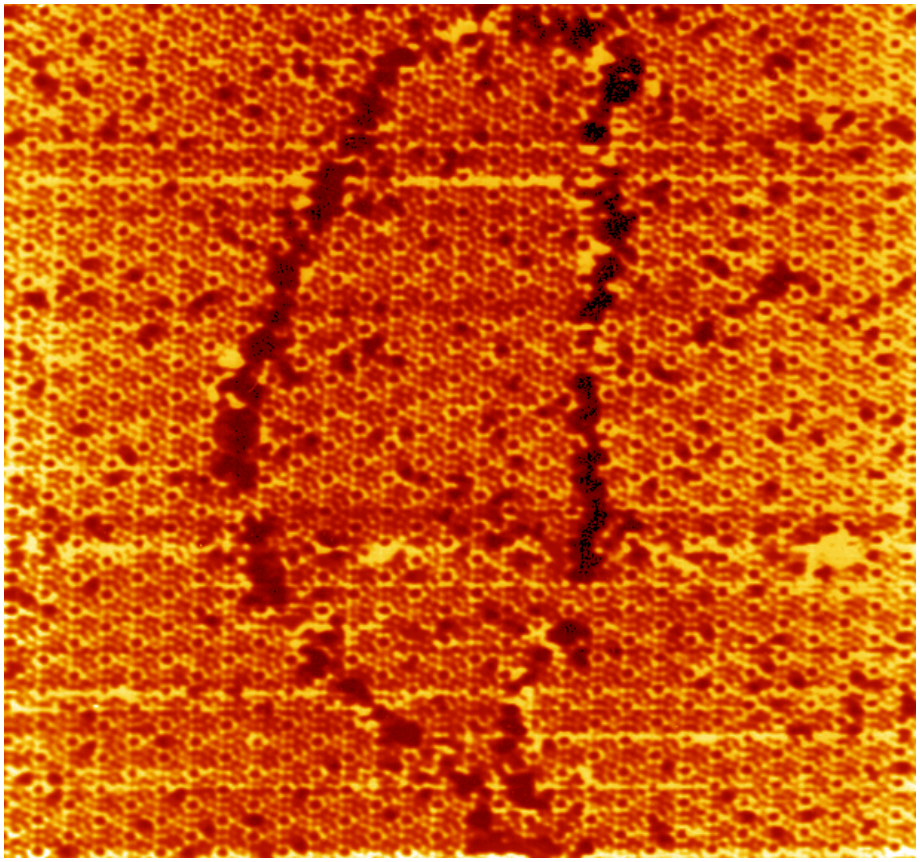

Electromigration

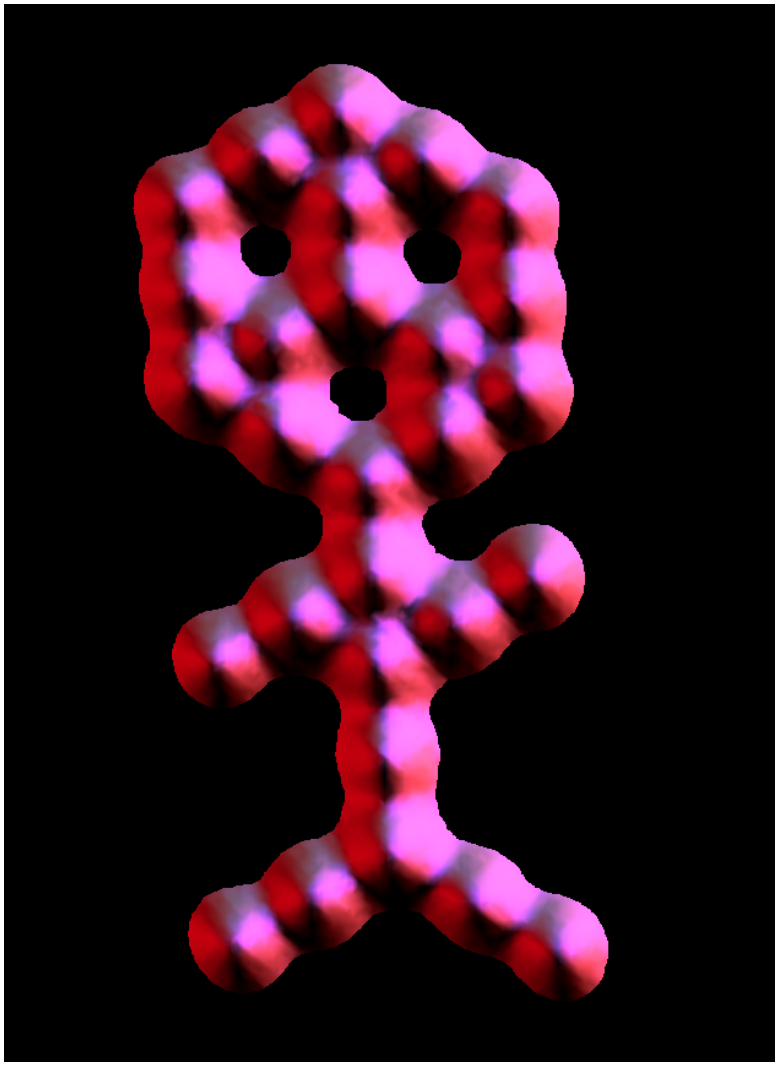

1. Direct interaction of effective charge on the defect with the electric field
2. 'Wind force' : scattering of electrons at defect (felt strongly by atoms closest to the junction)

CO on Pt(111)

4.5K UHV STM

Ch. Lutz, Eigler Lab, IBM

Atom Tracking

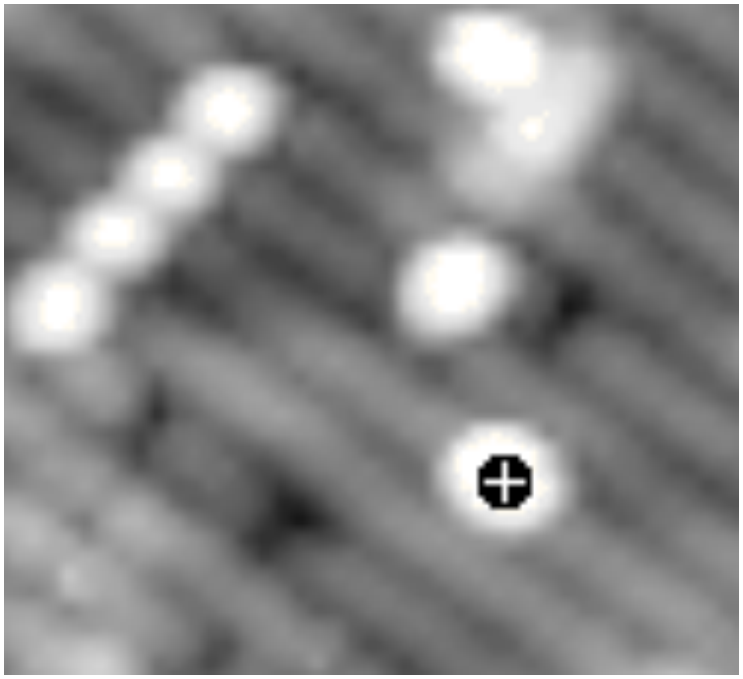

The atom tracker works by locking onto selected "bumps" (or "holes") using lateral feedback. The feedback maintains the position of the STM tip at the local maximum by continually climbing uphill. Once locked, atom-track data are acquired by reading the X, Y, and Z positions of the feedback electronics as a function of time. The motion of the surface feature is reflected in the coordinates of the atom tracker.

Inelastic Tunneling

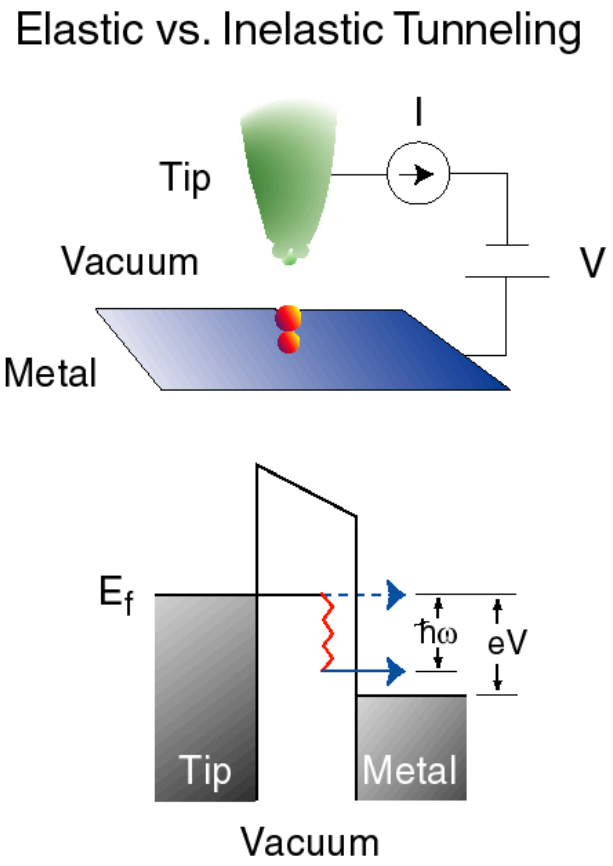

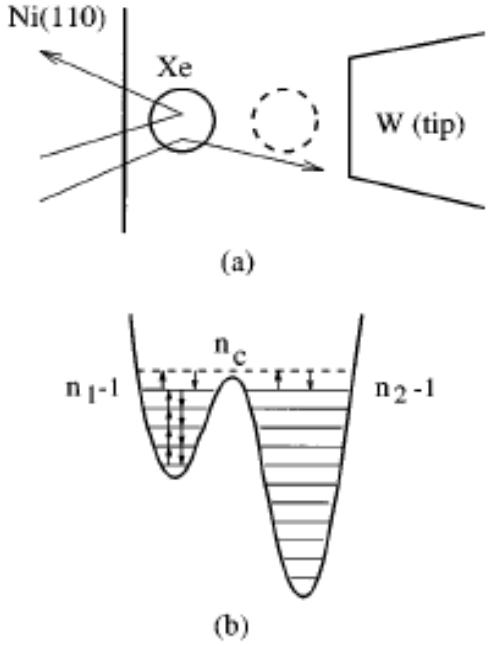

FIG. 1. (a) Schematic picture of the atomic switch. (b) Double-well model for atom transfer based on truncated harmonic oscillators. In the vibrational heating mechanism, the atom transfer results from stepwise vibrational excitation of the adsorbate-substrate bond by inelastic electron tunneling as depicted by arrows between the bound state levels of the adsorption well 1.

Reversible Rotation by Tunneling Electrons

Single Molecule Reversible Rotation

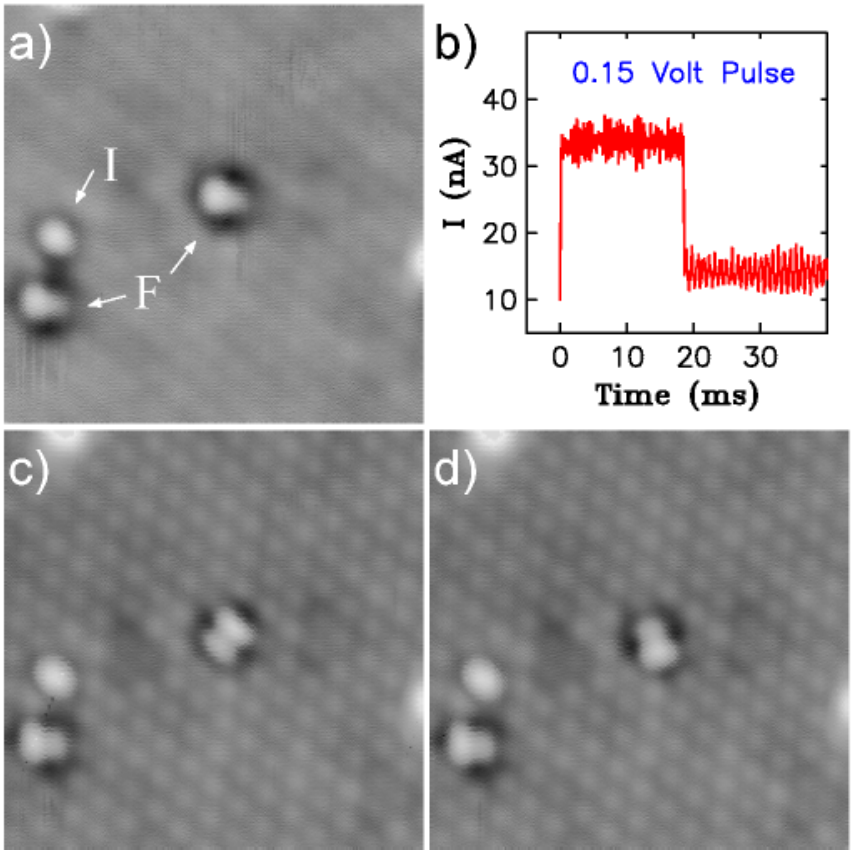

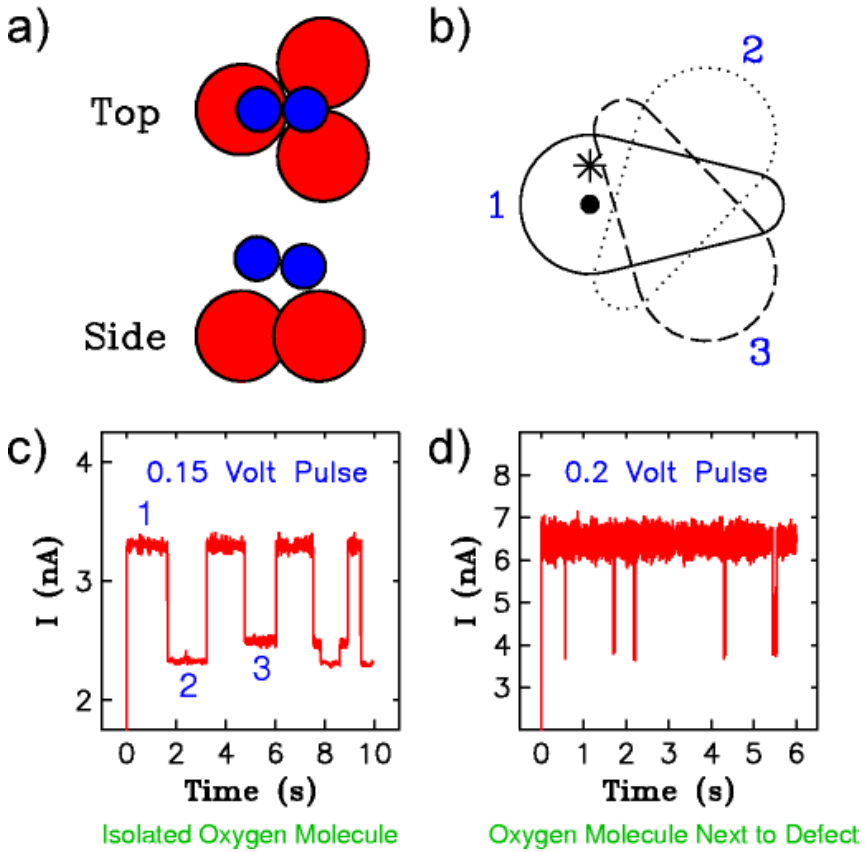

B. C. Stipe *et al.*,
SCIENCE 279, 1908 (1998)

(**A**) Schematic drawing showing top and side views of the fcc-site O2 molecule (black circles); Pt atoms are shown in gray. (**B**) Schematic outline of "pear" molecule shape as seen in STM images for each orientation. The solid dot is the position of maximum tip height for the first orientation; this is the tip position used for data collection. The asterisk shows an off-axis tip position displaced 0.4 Å from the solid dot. (**C**) Current during a 0.15-V pulse with the tip in the off-axis position in (B), showing three levels of current corresponding to the three orientations of the molecule. (**D**) Current during a 0.2-V pulse over a molecule next to an impurity showing a strong preference for a particular orientation.

Interaction between the probe and sample

Short-range:

1) Bonding

2) Repulsion

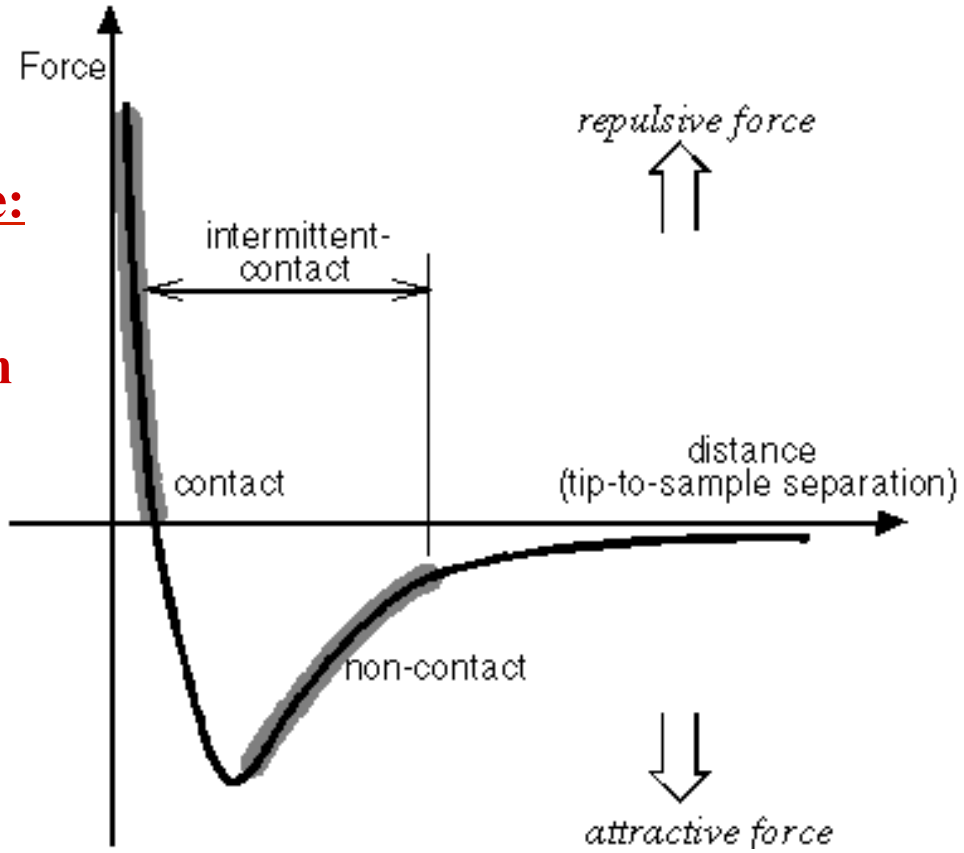

Long-range:

1) Van der Waal

2) Capillary

3) Magnetic

4) Electrostatic

Lennard-Jones potential $\phi(r) = - A/r^6 + B/r^{12}$

Atomic Image of Si(111)-(7×7) Taken with AFM

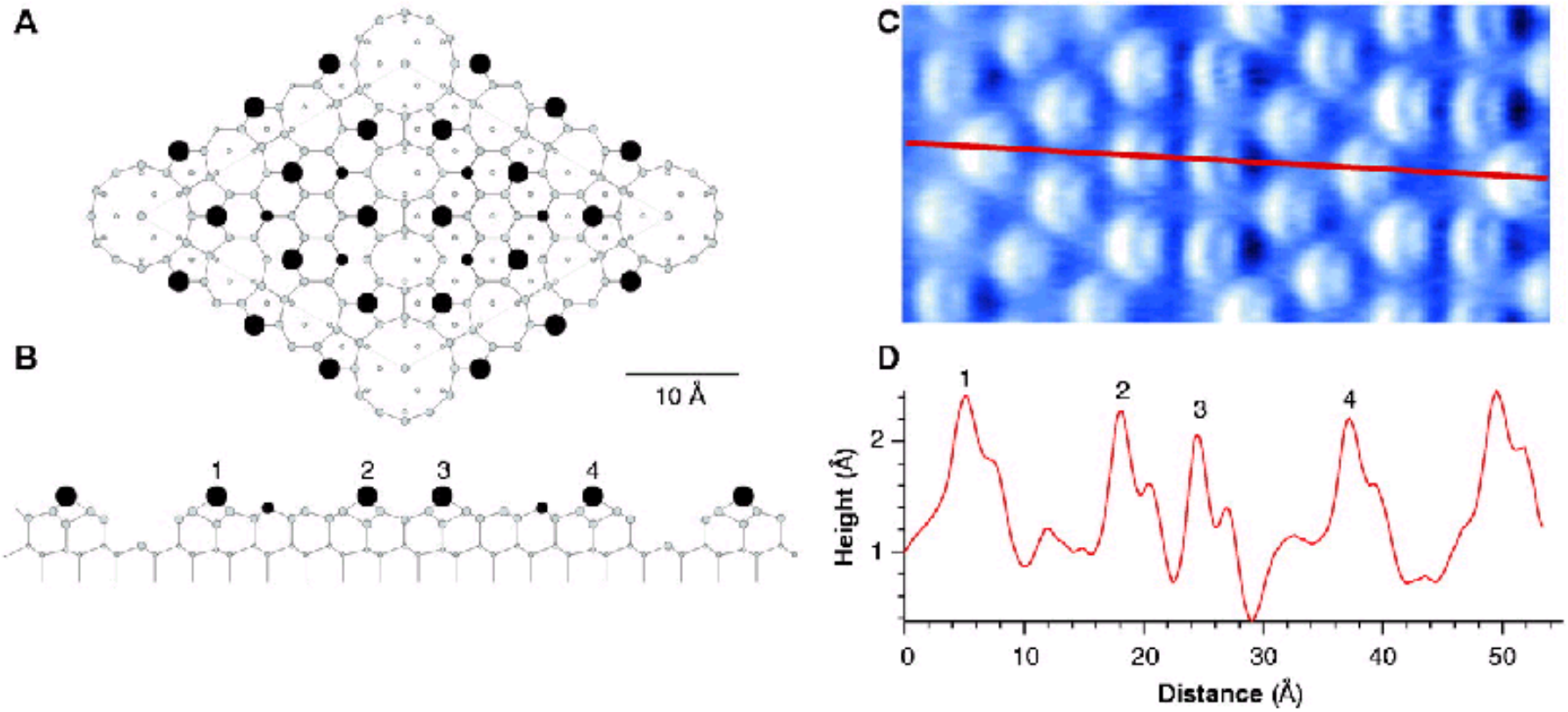

F.J. Giessibl *et al.*, Science 289, 422 (2000)

Chemical Structure of a Molecule

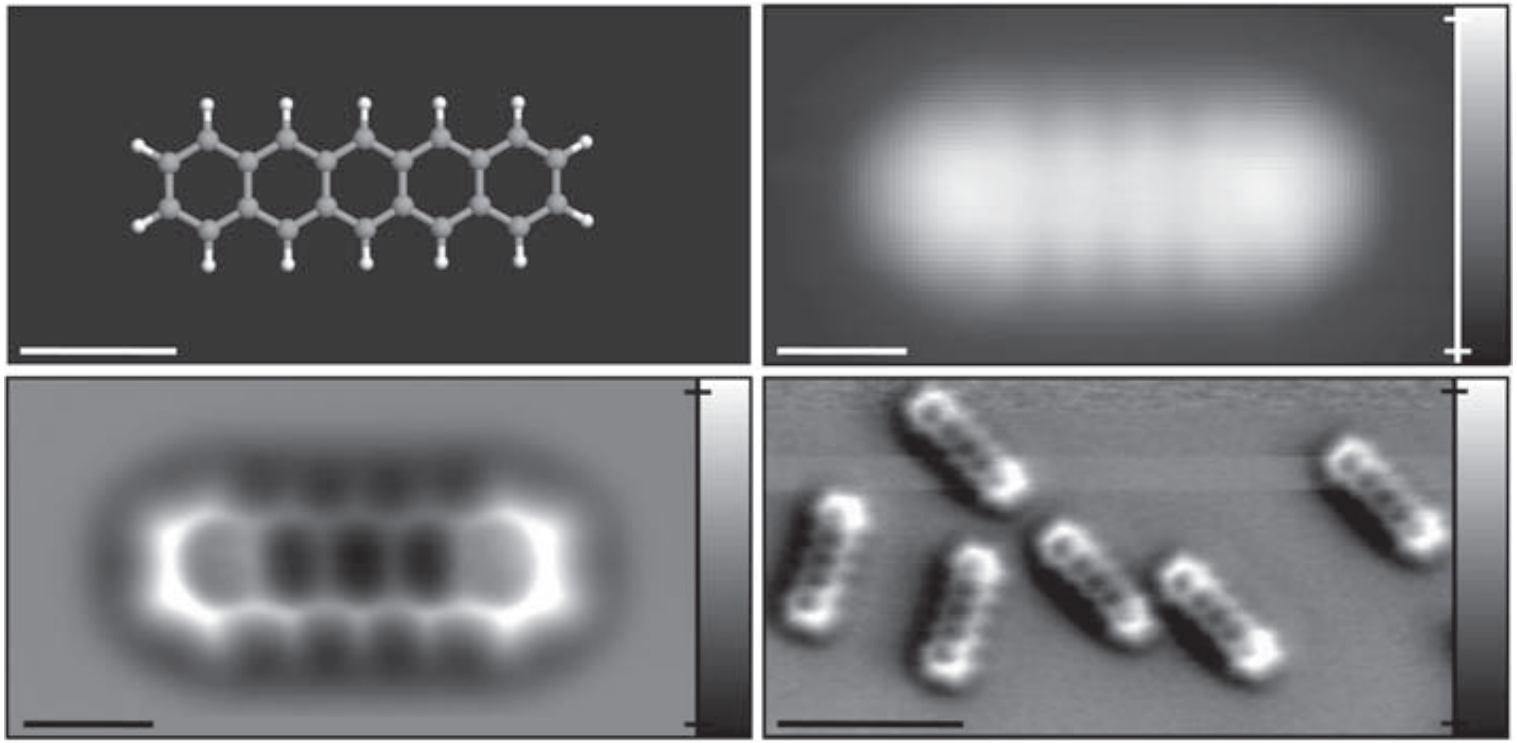

STM and AFM imaging of pentacene on Cu(111). (A) Ball-and-stick model of the pentacene molecule. (B) Constant-current STM and (C and D) constant-height AFM images of pentacene acquired with a CO-modified tip

L. Gross et al., Science 325, 1110 (2009)

Discriminating Chemical Bonds

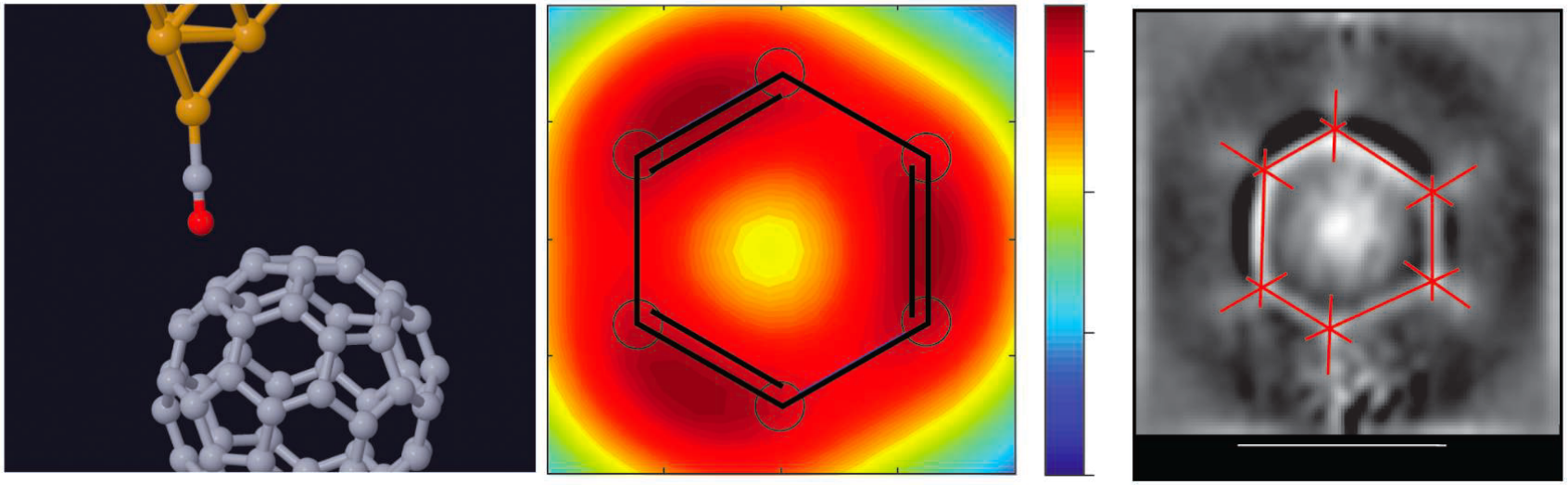

Forceful discrimination. Gross et al. used AFM with a CO-functionalized tip (A) to map the subtle differences in charge density (B) and bond length (C) associated with nonequivalent C-C bonds in a fullerene (C60) molecule and to correlate them with their bond order.

L. Gross et al., Science 337, 1326 (2012)

Nanolithography of Tapping-Mode AFM

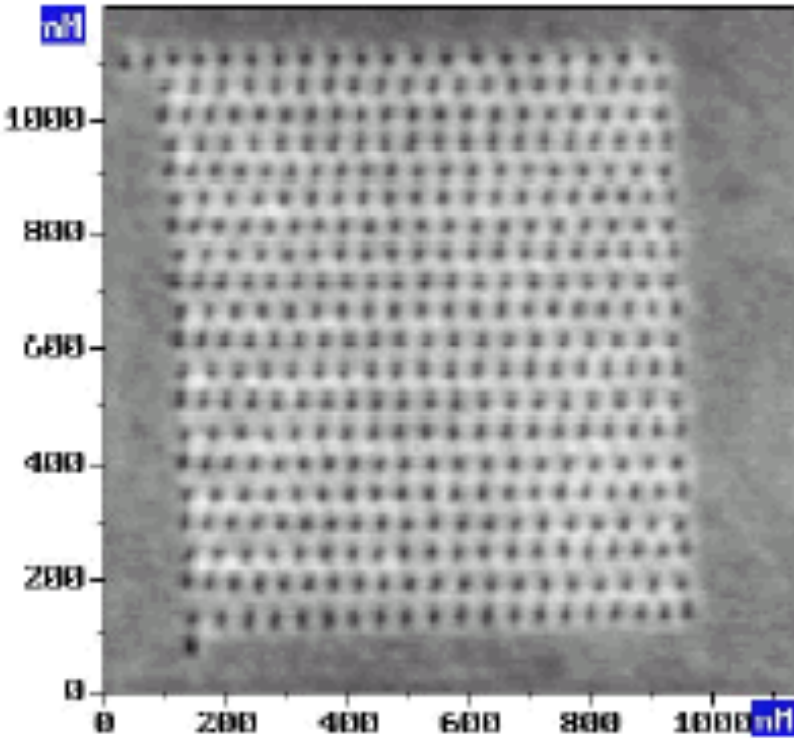

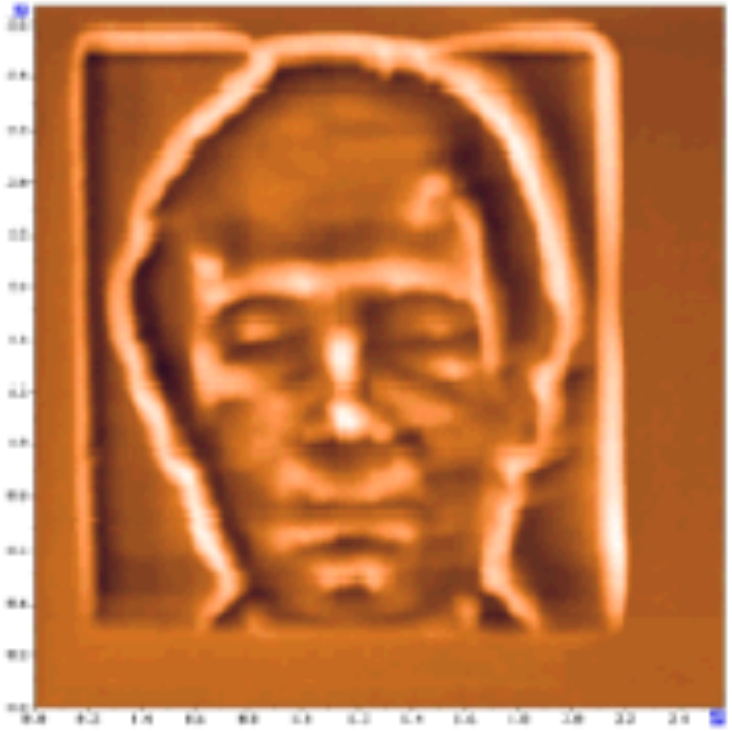

(1.2 μm× 1.2 μm)

(2.5 μm× 2.5 μm)

Image of polycarbonate film on silicon surface

7,000,000-YEAR-OLD SKULL: ANCESTOR? APE? OR DEAD END?

SCIENTIFIC AMERICAN

The Nose-Tickling Science of Bubbly

JANUARY 2003
WWW.SCIAM.COM

Micromachines Rewrite the Future of Data Storage

The NANODRIVE

PREDICTING EARTHQUAKES

FIGHTING CANCER WITH LIGHT

THE GOVERNMENT'S FLAWED DIET ADVICE

9 770036 873053 01
$4.95 U.K. £3.50

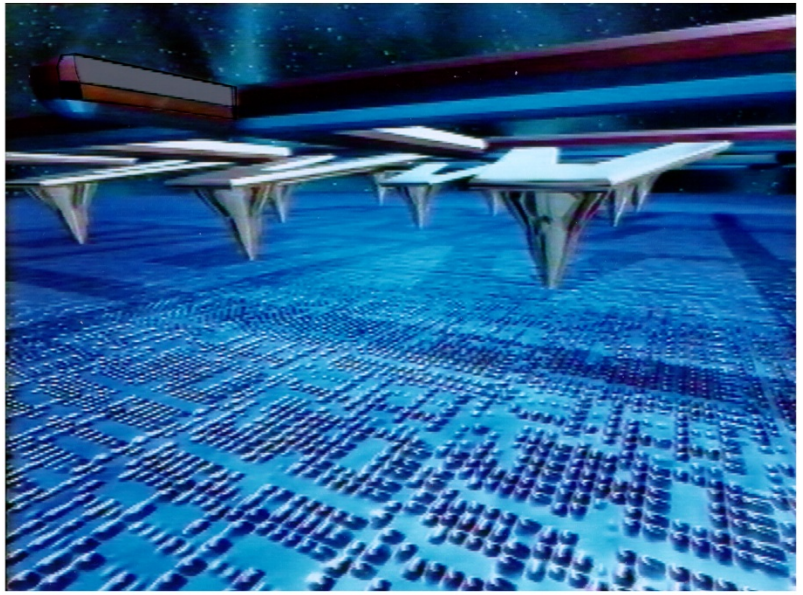

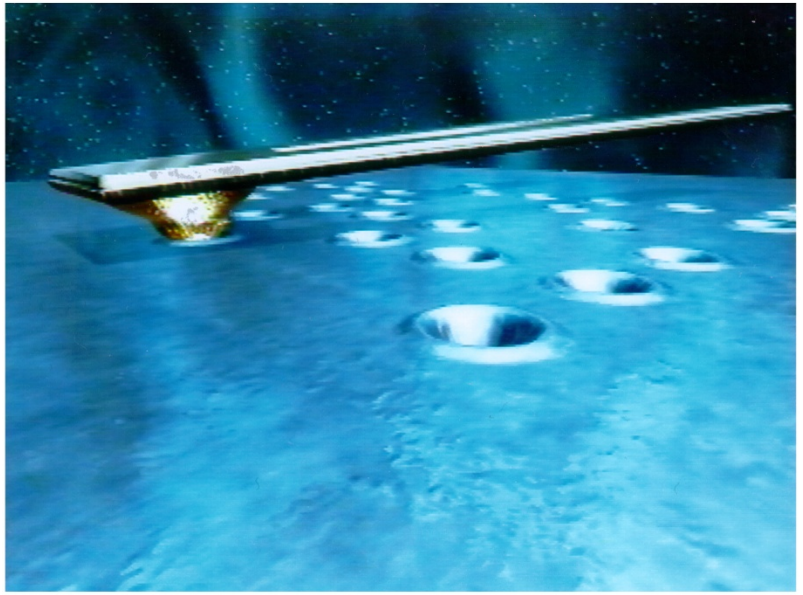

"MILLIPEDE"

Highly parallel, very dense AFM data storage system

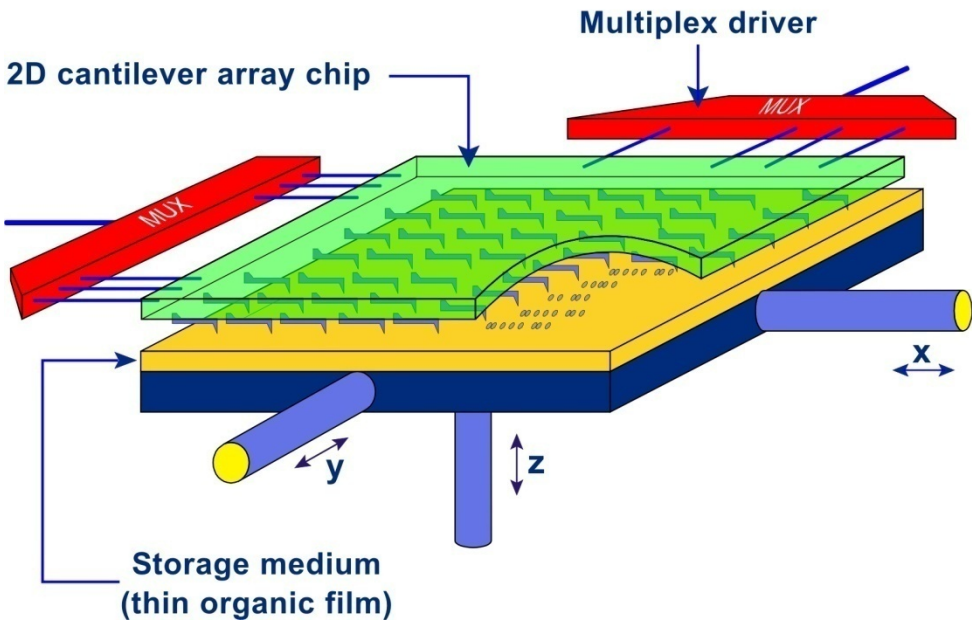

The Millipede concept: for operation of the device, the storage medium - a thin film of organic material (yellow) deposited on a silicon "table" - is brought into contact with the array of silicon tips (green) and moved in x- and y-direction for reading and writing. Multiplex drivers (red) allow addressing of each tip individually.

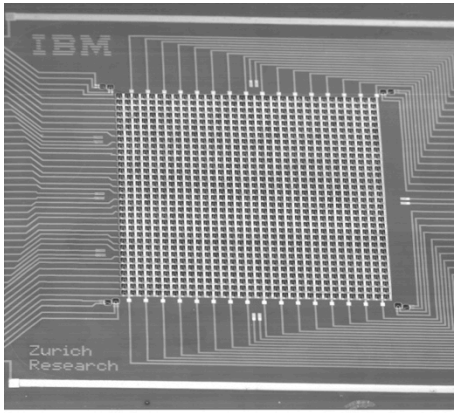

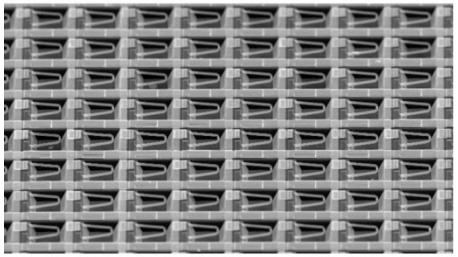

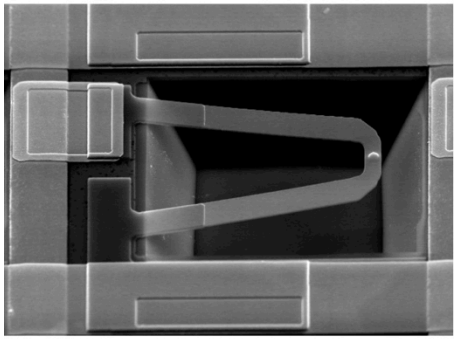

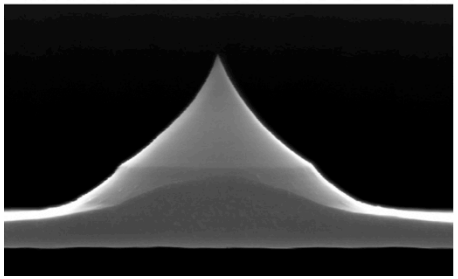

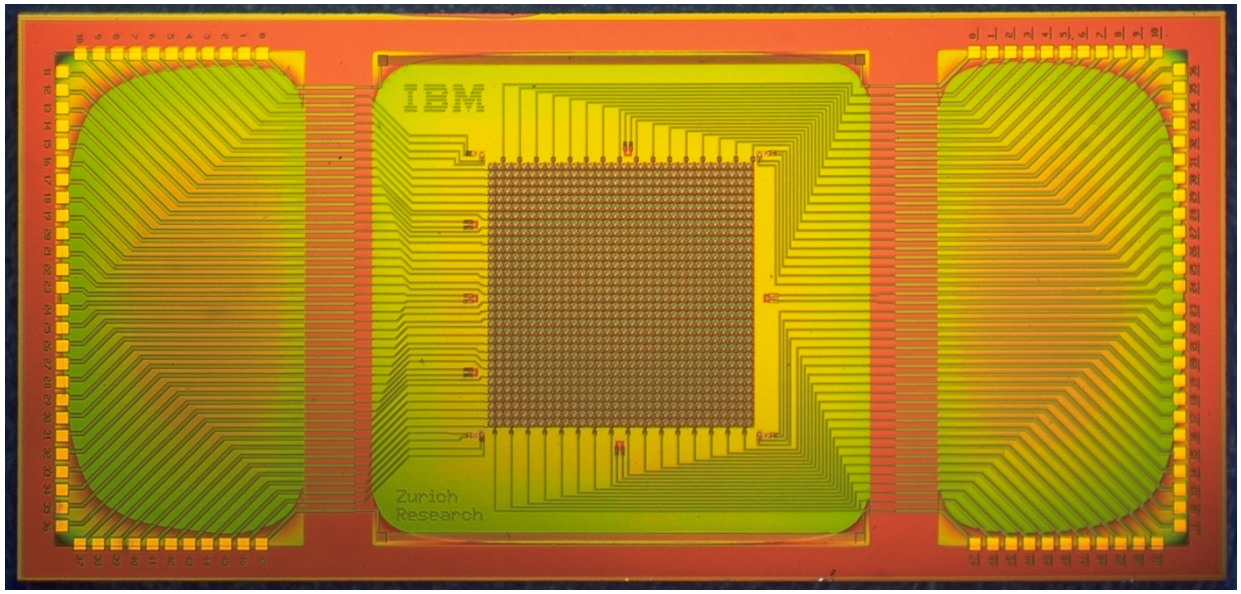

The Millipede chip: the image shows the electrical wiring for addressing the 1,024 tips etched out in a square of 3mm by 3mm (center). The chip's size is 7 mm by 14 mm.

Millipede cantilevers and tips: electron microscope views of the 3 mm by 3 mm cantilever array (top), of an array section of 64 cantilevers (upper center), an individual cantilever (lower center), and an individual tip (bottom) positioned at the free end of the cantilever which is 70 micrometers (thousands of a millimeter) long, 10 micrometers wide, and 0.5 micrometers thick. The tip is less than 2 micrometers high and the radius at its apex smaller than 20 nanometers (millionths of a millimeter).

Nano-Lithography with an AFM Tip

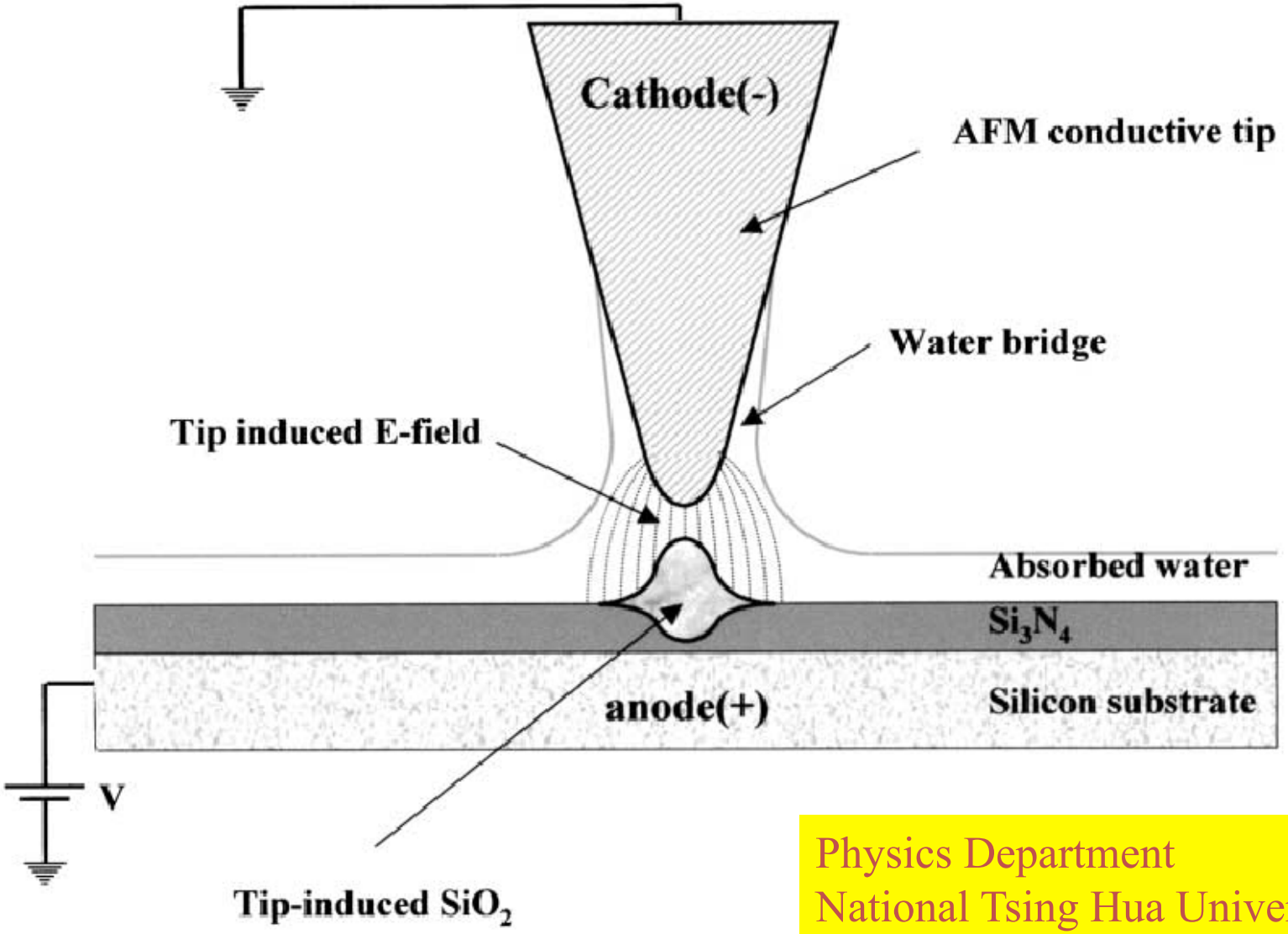

Physics Department
National Tsing Hua University

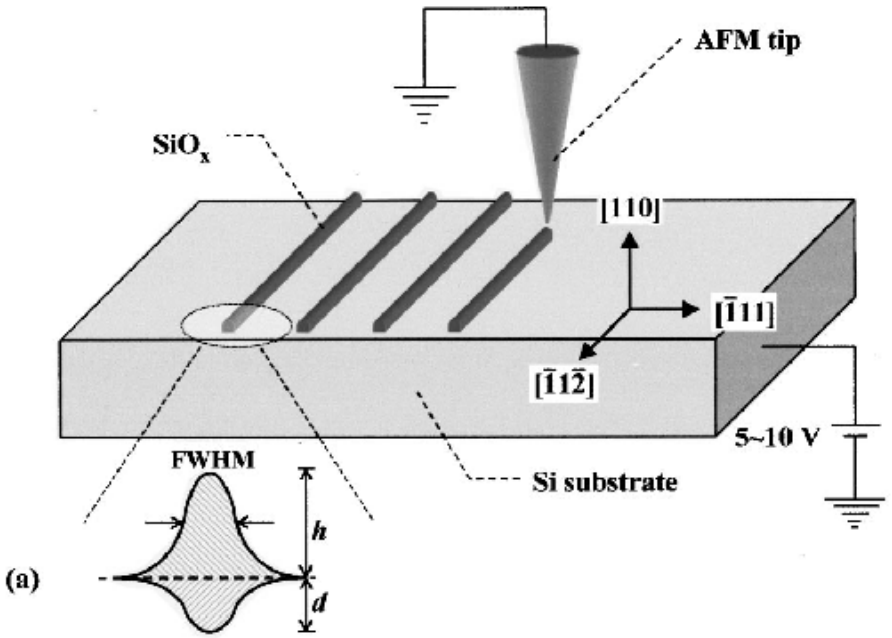

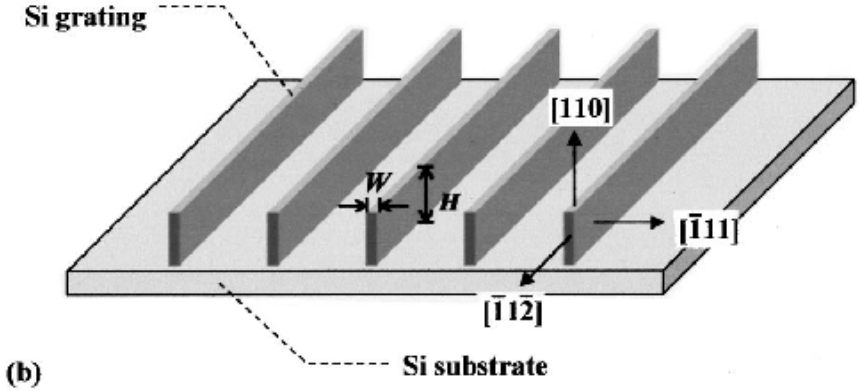

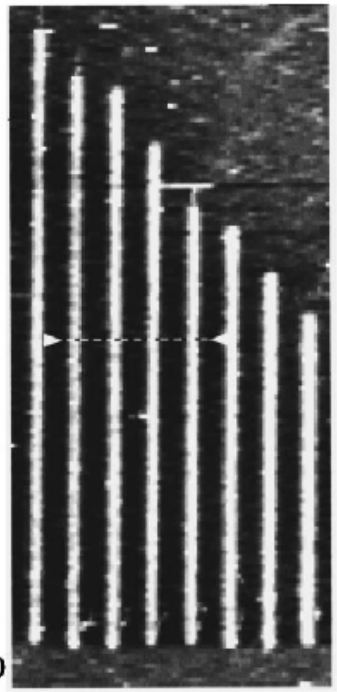

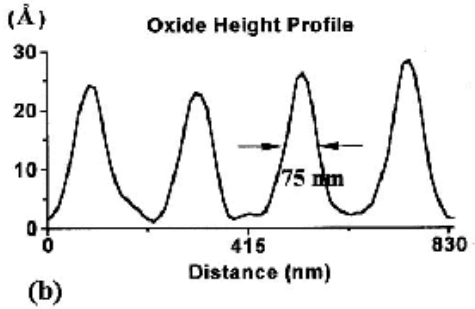

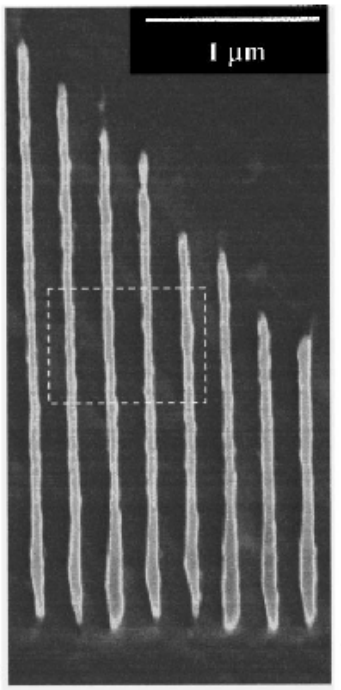

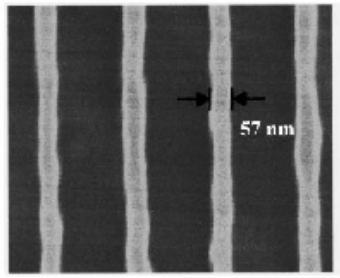

F.S.-S. Chien *et al.*, APL 75, 2429 (1999)

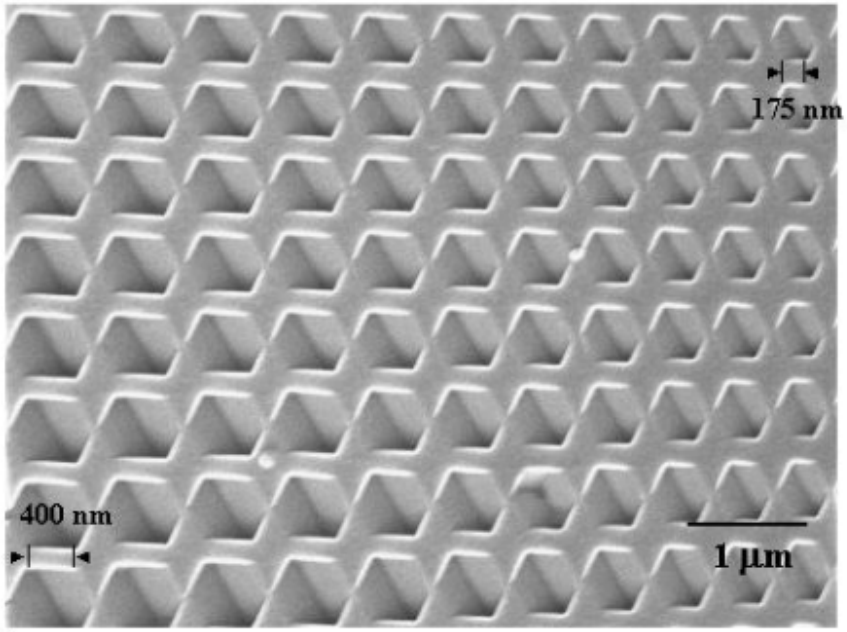

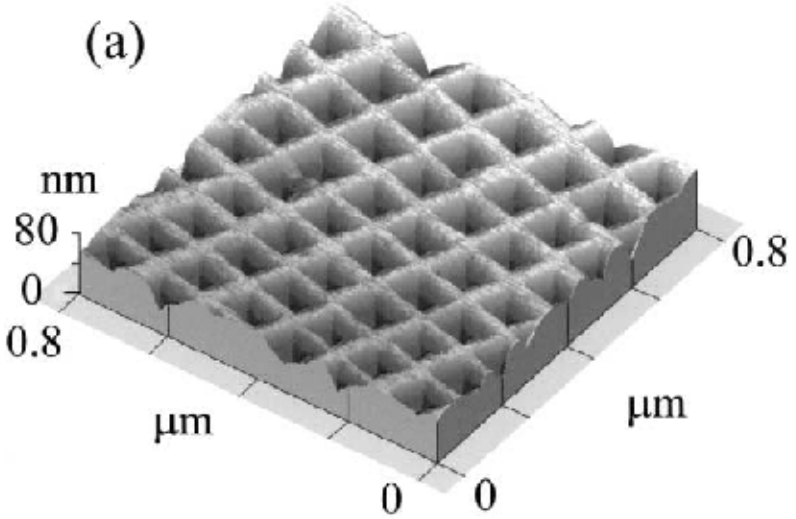

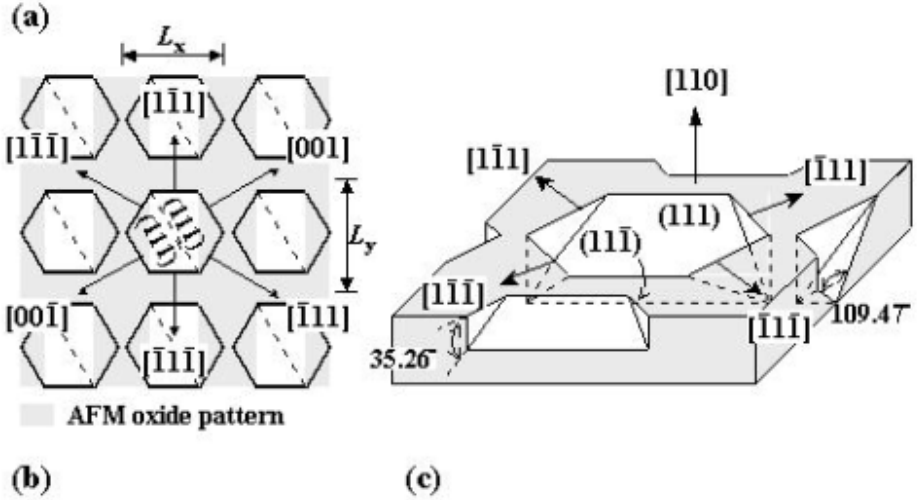

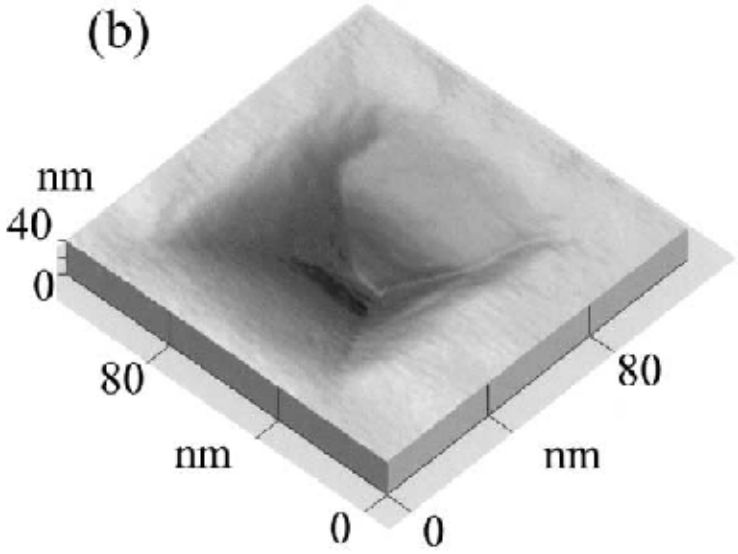

果尚志 , Physics Dept., National Tsing Hua University

Setup for an Optical Tweezer

An **optical tweezer** is a scientific instrument that uses a focused laser beam to provide an attractive or repulsive force, depending on the index mismatch (typically on the order of piconewtons) to physically hold and move microscopic dielectric objects. Optical tweezers have been particularly successful in studying a variety of biological systems in recent years.

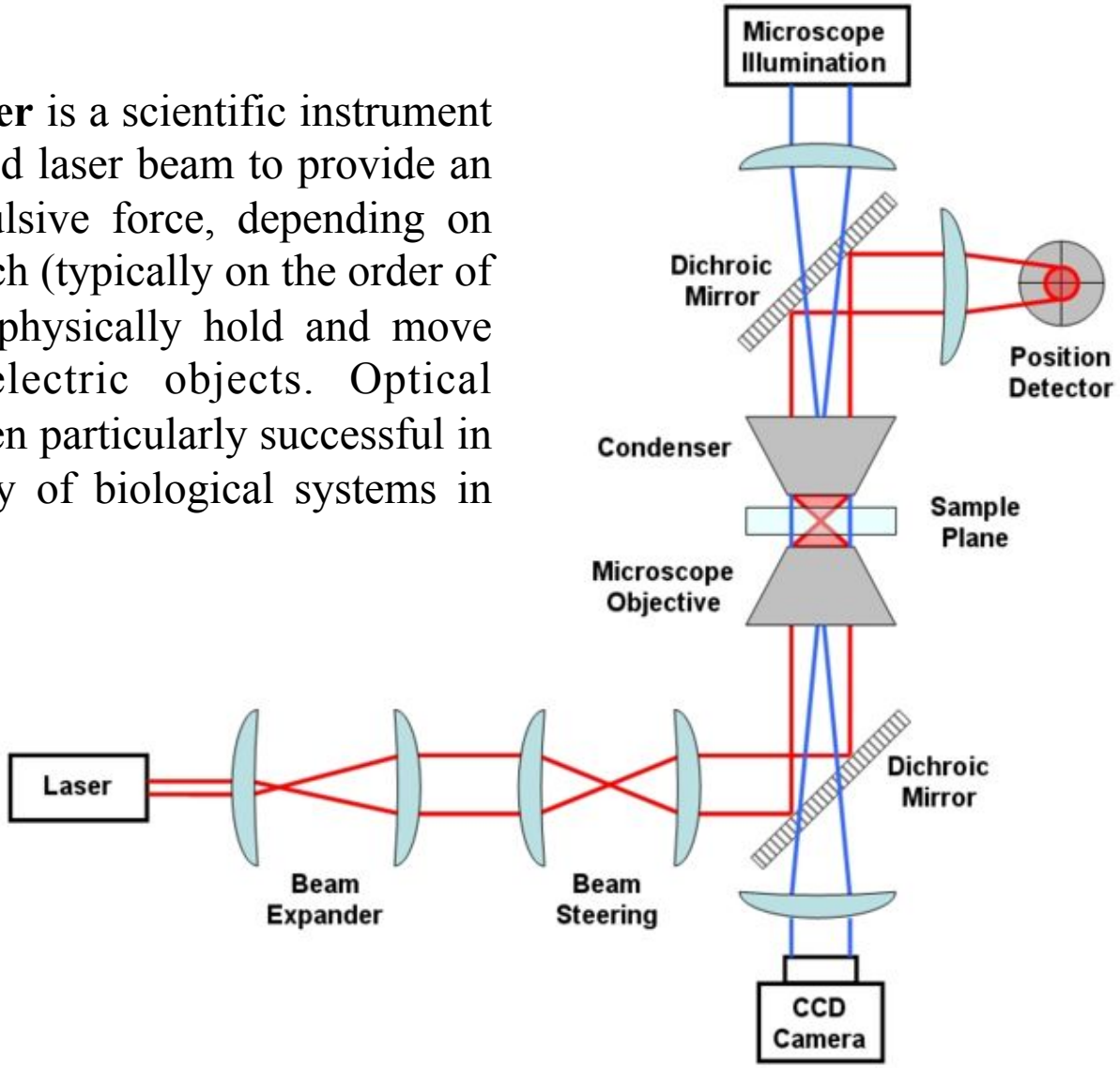

Optical scattering force

- each absorption results in a well-defined impulse
- isotropic spontaneous emission causes no average recoil
- average scattering force is therefore

$$\mathbf{F} = n\hbar\mathbf{k}$$

where n is photon absorption rate

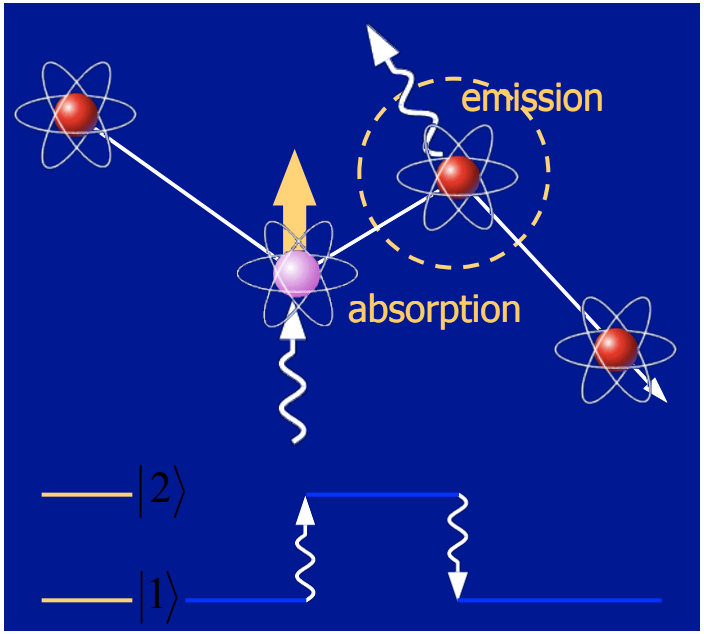

Working Principles of Optical Tweezer

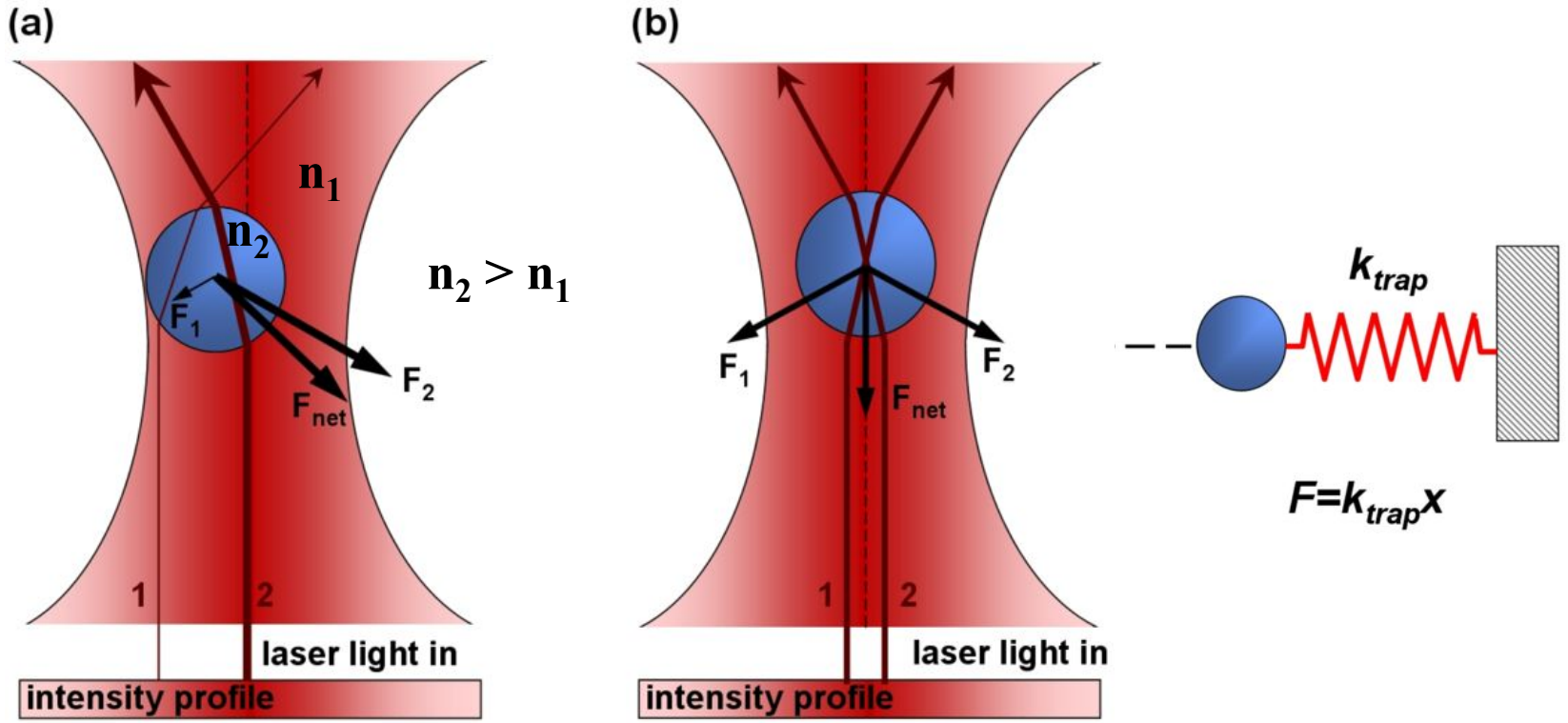

A particle encountering the laser beam will be pushed towards the center of the beam, if the particle's index of refraction is higher than that of the surrounding medium. In a ray optics picture we realize how light is deflected in the particle, resulting in a gradient force that pushes the particle vertically to the propagation of the laser beam, towards the largest intensity of light (the middle of the laser beam). By focusing the light, the gradient force pushes the particle backwards as well. If this force overcomes the propagation force of the laser beam, the particle is trapped.

Optical Tweezer on a Plastic Bead

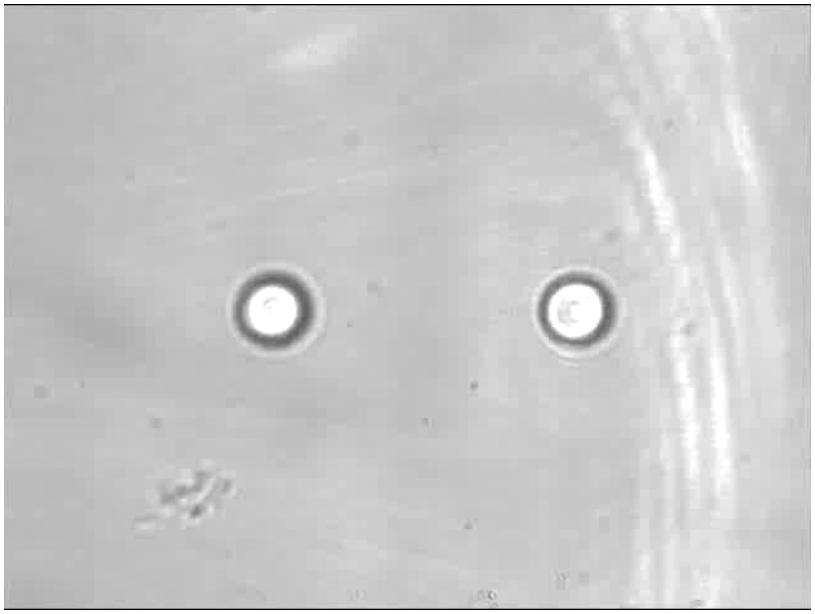

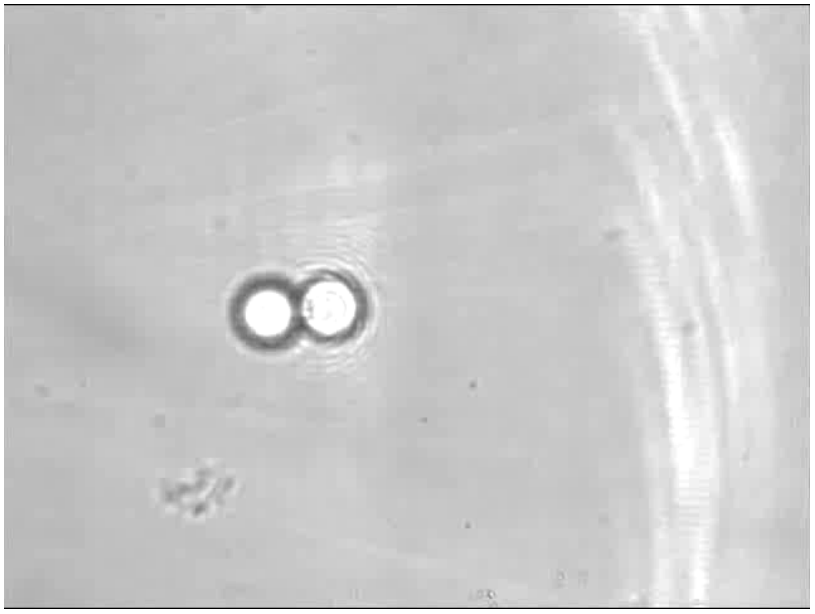

Magnetic Tweezer

A *Magnetic Tweezer* is a scientific instrument for exerting and measuring forces on magnetic particles using a magnetic field gradient. Typical applications are single-molecule micromanipulation, rheology of soft matter, and studies of force-regulated processes in living cells. Forces are typically on the order of pico- to nanonewtons. Due to their simple architecture, magnetic tweezers are one of the most popular and widespread biophysical techniques.

$$\mathbf{F} = \nabla(\mathbf{m} \cdot \mathbf{H})$$

$$\tau = \mathbf{m} \times \mathbf{H}$$

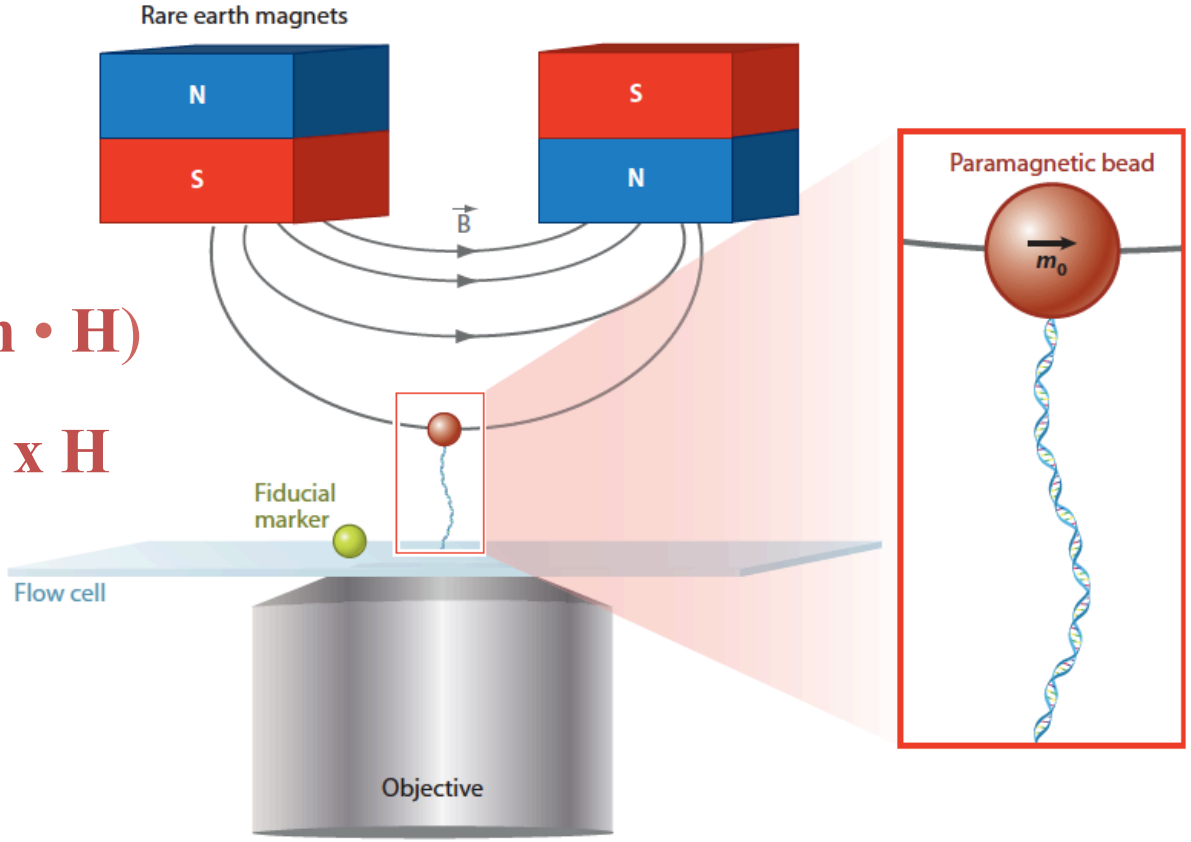

Working Principles of Magnetic Tweezer

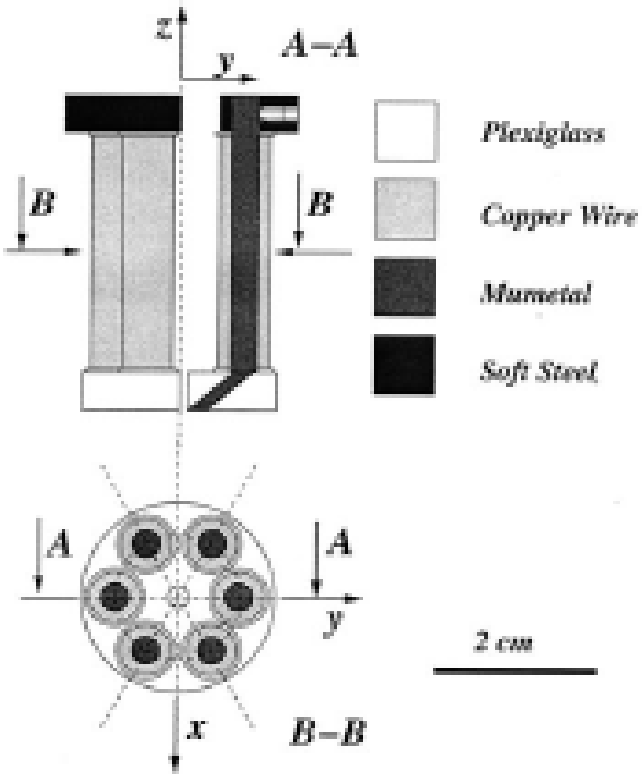

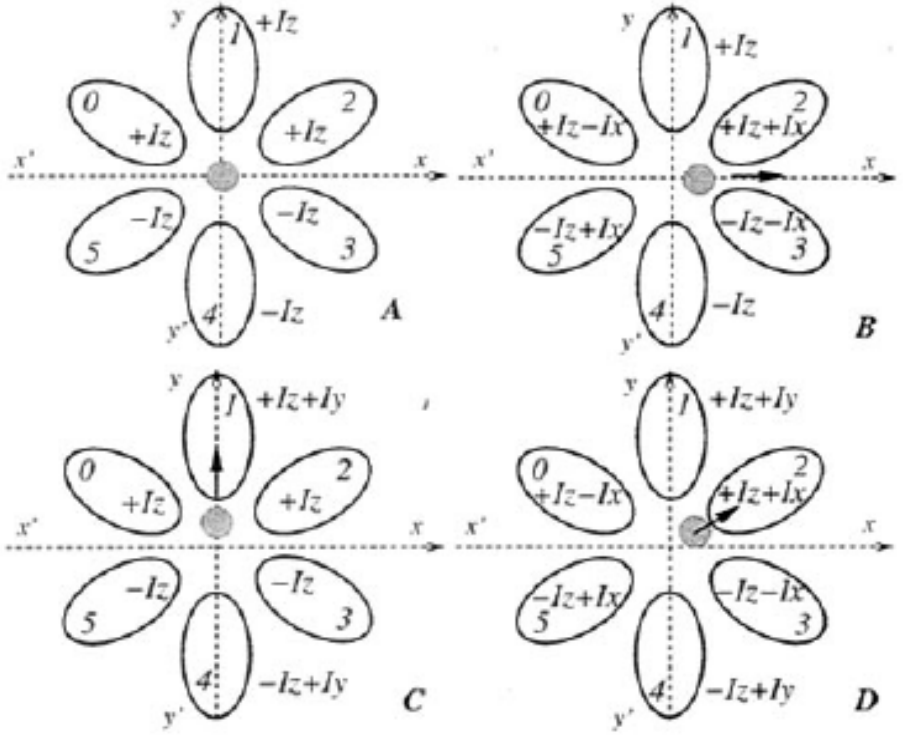

FIGURE 4 Schematic representation of the principles governing the bead displacement (top view of the sample). (*A*, *B*, and *C*) Three different current configurations are used to move the magnetic particle along *z*, *x*, and *y*. (*D*) More complicated displacements can be reached by linear combination of the basic settings. Note that, in this figure, all the currents (I_x, I_y, and I_z) are positive.

Charlie Gosse and Vincent Croquette
Biophysical Journal **82** (2002) 3314.

Engineering CNT with e-beam

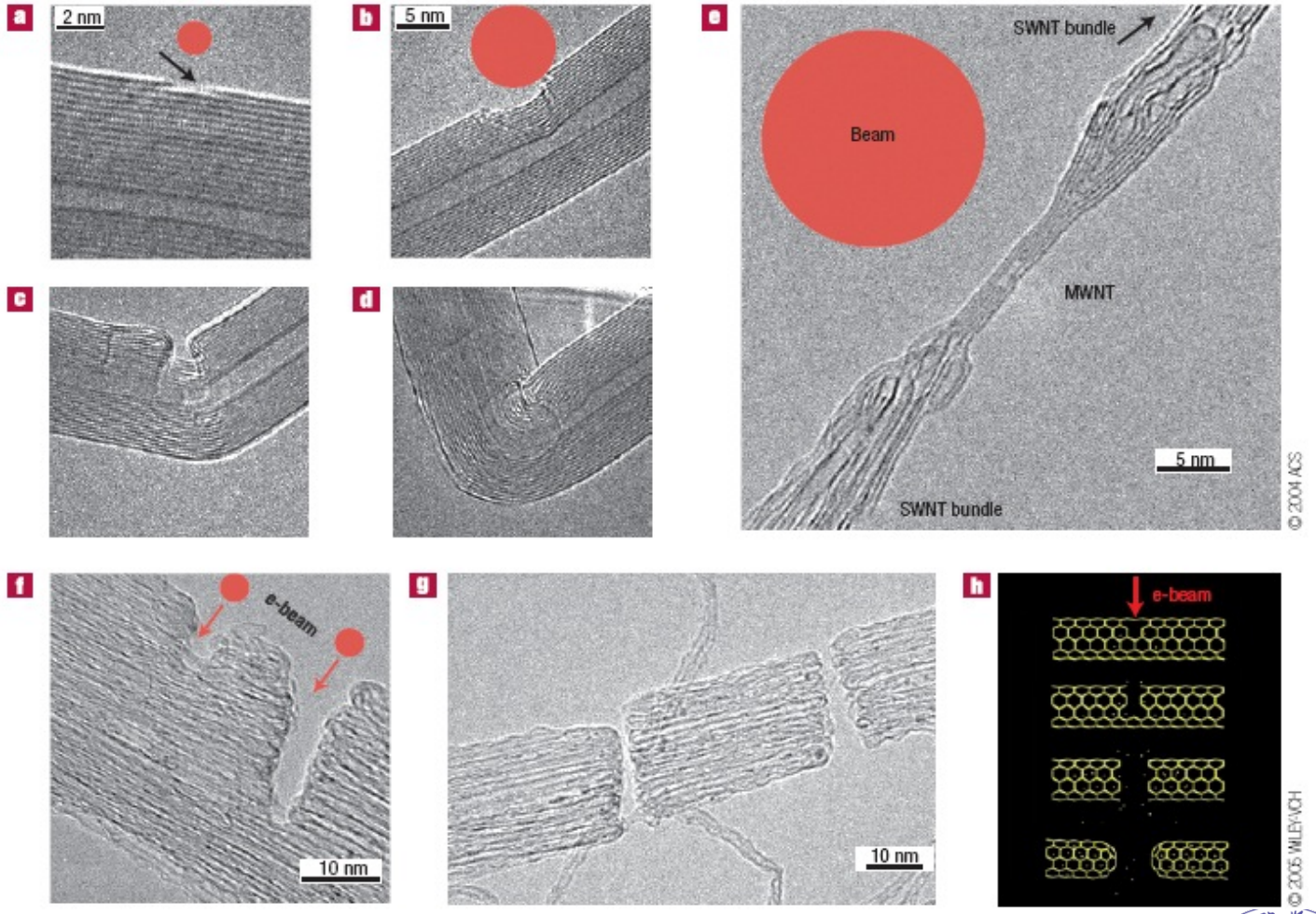

A.V. Krasheninnikov and F. Banhart
Nature Materials **6**, 723 (2007)

Peeling the nanotube from inside